M. Quack and G. Seyfang, Tunnelling and Parity Violation in Chiral and Achiral Molecules :Theory and High Resolution Spectroscopy, Chapter 6 in ' Tunnelling in Molecules: Nuclear Quantum Effects from Bio to Physical Chemistry ' J. Kästner and S.Kozuch eds. Royal Society of Chemistry , Cambridge, England (2020) pp 192-244

CHAPTER 6

Tunnelling and Parity Violation in Chiral and Achiral Molecules: Theory and High-resolution Spectroscopy

MARTIN QUACK* AND GEORG SEYFANG

ETH Zürich, Laboratory for Physical Chemistry, CH-8093 Zürich, Switzerland
*Email: Martin@Quack.ch

6.1 Introduction

Quantum mechanical tunnelling was discovered in 1927 by Friedrich Hund in the context of a discussion of the stereomutation reaction between the enantiomers of chiral molecules. We review here the fundamental new aspects introduced by the discovery of parity violation in 1957 and the subsequent formulation of the standard model of particle physics (SMPP), which led to a radical change in our understanding of the dynamics of stable chiral molecules. We first review the basic theory of parity violation in the framework of the SMPP with the discovery of a new order of magnitude for chiral molecules. We then discuss the conceptual changes for the quantum dynamical tunnelling of achiral, transiently chiral and stable chiral molecules with several current examples. We summarize the current status of the theory. We then outline the concepts for experiments and summarize the current status of experiment.

When Friedrich Hund in 1927[1–3] investigated for chiral molecules the spectroscopic and kinetic consequences of the then-new theory of quantum

Theoretical and Computational Chemistry Series No. 18
Tunnelling in Molecules: Nuclear Quantum Effects from Bio to Physical Chemistry
Edited by Johannes Kästner and Sebastian Kozuch

Published by the Royal Society of Chemistry, www.rsc.org

mechanics as just formulated in terms of the Heisenberg equations of motion[4–6] and the Schrödinger equation, which had been found by Erwin Schrödinger during a skiing holiday in Arosa over the Christmas and New Year holiday 1925/26,[7–13] he discovered a strange phenomenon: For symmetry reasons the ground state wave function as an eigenstate of the Schrödinger equation must have a well-defined "parity" as symmetry with respect to the inversion at the potential maximum in the double-well potential, which could be used in a simple one-dimensional description of the stereomutation reaction interconverting the enantiomers of chiral molecules (Figure 6.1).

More generally this symmetry of parity is related to the inversion of the three spatial coordinates *x, y, z*, of a physical system (Figure 6.2). Therefore the probability distribution related to the ground state wave function (χ_+ for positive parity in Figure 6.1) had to be delocalized. The first excited state ($-\chi_-$ in Figure 6.1) of negative parity and antisymmetric with respect to inversion would be separated by a small energy interval $\Delta E_\pm = E_- - E_+$ from the ground state. Both eigenstates would have to be considered as achiral. However, a superposition of these states ($\chi_+ + \chi_-$) and ($\chi_+ - \chi_-$) would generate wave functions λ and ρ, localized and chiral, as observed in common experiments of chemistry. These localized states and probability distributions would interconvert λ to ρ and back in a half period of the periodic motion with period τ:

$$t_{\lambda\to\rho} = \tau/2 = h/(2\Delta E_\pm) \tag{6.1}$$

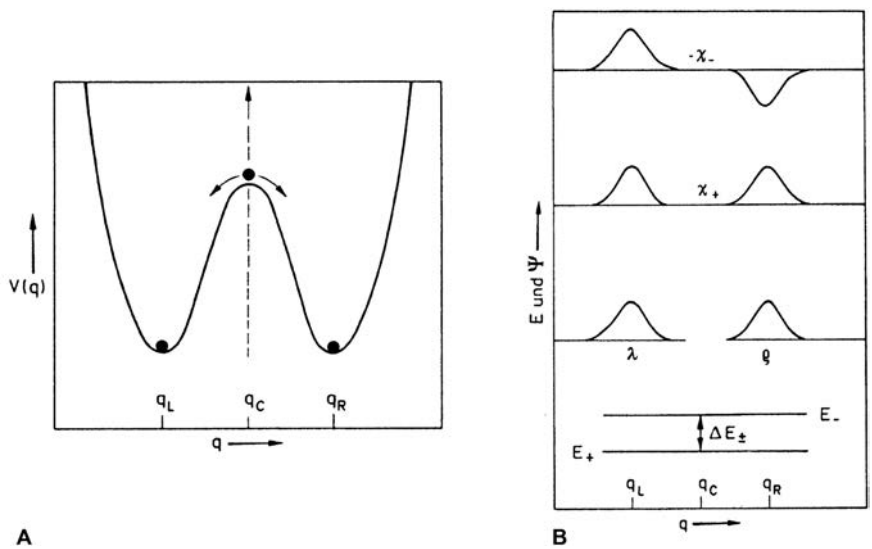

Figure 6.1 The double minimum potential for illustrating symmetry breaking in classical dynamics (A) and parity symmetry, localization and tunnelling in quantum dynamics. Wave functions are shown in (B).
Reproduced from ref. 157 with permission from World Scientific Publishing, Copyright 1995.

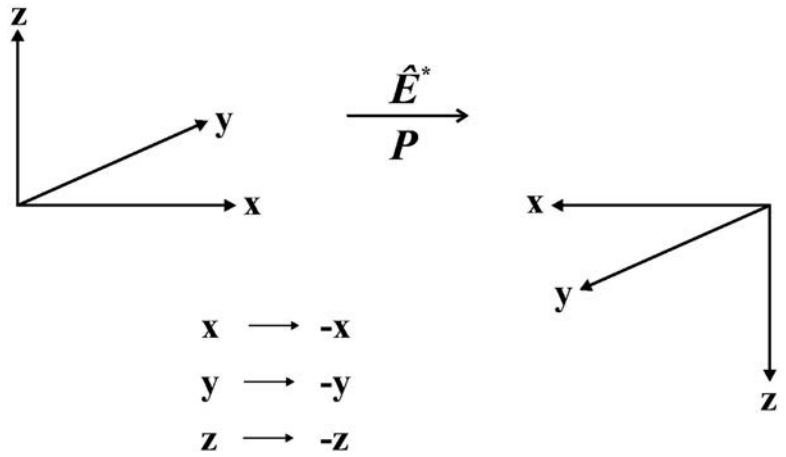

Figure 6.2 Reflection E^* or parity ($\hat{P}$) operation.
Adapted from ref. 36 with permission from John Wiley and Sons, © 2002 WILEY-VCH Verlag GmbH & Co. KGaA, Weinheim.

where h is Planck's constant, although both energies E_+ and E_- were much smaller than the barrier heights considered for chiral molecules. Thus the reaction of this quantum mechanical system could happen at energies below the barrier for reaction, a process impossible, even unthinkable of, in classical mechanics. Later this effect was called tunnelling or the tunnel effect, with the picture of a process that could happen as if there were a "tunnel" through the barrier (see ref. 14 and 15 for more of the history). Hund's description, which is also applicable to achiral molecules such as NH_3, which can be described by a similar double-well potential, has entered the textbooks, and the quantum mechanical tunnel effect has since then been observed in numerous areas of physics and chemistry and has been subject of many books, including the present book[16] (see ref. 17–21 to give just a few examples). In classical mechanics the symmetrical state of the system is located at the maximum of the potential, a point of unstable equilibrium, the stable states at the minima being strictly localized and degenerate, as indicated in Figure 6.1A, very different from the quantum mechanical description.

The discovery of parity violation in 1956/57[22–26] led to consequences for the tunnelling dynamics of chiral molecules that have not yet widely entered the textbooks of chemistry (see, however, ref. 27 and 28). The present brief review deals with these new aspects of tunnelling in chiral molecules as well as related aspects in achiral molecules. Our aim is here to provide a conceptual summary of these phenomena both concerning theoretical and experimental aspects. For more detailed reviews, from which we draw in particular (and in part literally), we refer to ref. 14, 15, 27–32. We shall first briefly outline the theory of parity violation in the framework of the Standard Model of Particle Physics, SMPP, following mainly ref. 27–35.

6.2 Parity Violation in Chiral Molecules in the Framework of the SMPP

6.2.1 Introductory Remarks

In the introduction to his famous paper ''Quantum Mechanics of Many Electron Systems'' Paul Adrien Maurice Dirac wrote one of the most cited sentences in quantum chemistry:[37]

''The underlying physical laws for the mathematical theory of a large part of physics and the whole of chemistry are thus completely known and the difficulty is only that the exact application of these laws leads to equations much too complicated to be soluble. It therefore becomes desirable that approximate practical methods of applying quantum mechanics should be developed, which can lead to an explanation of complex atomic systems without too much computation''.

It is remarkable that the second part of this statement, which forms a reasonable starting point for modern, approximate numerical quantum chemistry and computational chemistry, is only rarely cited. The more frequently cited first sentence with the strong statement about understanding ''the whole of chemistry'' and the small restriction ''the difficulty is only'', which claims that the quantum physics of the first half of the 20th century contains all basic knowledge about chemistry, is the one that seems to be liked by many theoretical chemists and physicists. It turns out, however, that this statement is incorrect. There is at least one important part of chemistry, namely stereochemistry and molecular chirality, which can be understood properly only when including the parity-violating weak nuclear force in our quantum chemical theory in the framework of what we have termed ''electroweak quantum chemistry'',[33,34] completely and fundamentally unknown at the time of Dirac's statement.[37]

Figure 6.3 summarizes the modern view of the origin of the fundamental interactions as publicized on the website of a large accelerator facility (CERN[38]). According to this view, the electromagnetic force, which is included in ''Dirac-like'' ordinary quantum chemistry, leads to the Coulomb repulsion, say, between two electrons in a molecule by means of photons as field particles. In the picture the two electrons are compared to the ladies on two boats throwing a ball. If we do not see the exchange of the ball, we will observe only the motion of the boats resulting from the transfer of momentum in throwing the ball, and we could interpret this as resulting from a repulsive ''force'' between the two ladies on the boats. Similarly, we interpret the motion of the electrons resulting from ''throwing photons as field particles'' as arising from the Coulomb law, which forms the basis of ordinary quantum chemistry. The Coulomb force with the $1/r$ potential energy law is of long range. The other fundamental forces arise similarly, but with other field particles. The strong force with very short range (0.1–1 fm) mediated by the gluons is important in nuclear physics but has only indirect influence in chemistry by providing the structures of the nuclei, which enter as

The forces in nature			
Type	Intensity of forces (decreasing order)	Binding particle (field quantum)	Important in
Strong nuclear force	~1	Gluons (no mass)	Atomic nucleus
Electro-magnetic force	$\sim 10^{-3}$	Photons (no mass)	Atoms and molecules
Weak nuclear force	$\sim 10^{-5}$	Bosons Z, $W+$, $W-$, (heavy)	Radioactive β-decay, chiral molecules
Gravitation	$\sim 10^{-38}$	Gravitons (?)	Sun and planets, *etc.*

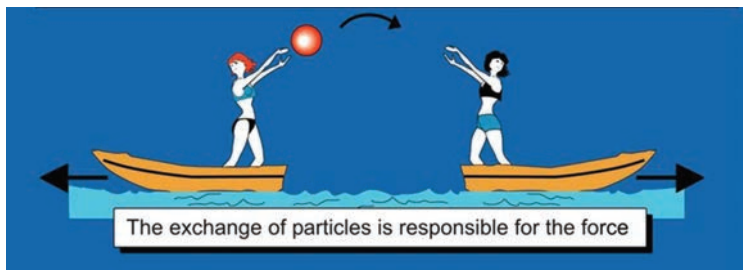

Figure 6.3 Forces in the standard model of particle physics (SMPP) and important effects. This is taken from the CERN website ref. 38, but the importance of the weak interaction for chiral molecules has been added here from our work.
Reproduced from ref. 29 with permission from the Royal Society of Chemistry, in turn, adapted from ref. 38, Public Domain. (We note that, while not referred to in ref. 38, the motif of the lightly dressed ladies throwing balls can be found in a mosaic at Piazza Armerina. Sicily, from the 4th century AD).

parameters in chemistry, but there is otherwise usually no need to retain the strong force explicitly in chemistry. The weak force, on the other hand, is mediated by the $W^{\pm}$and Z^0 Bosons of very high mass (86.316 and 97.894 Dalton, of the order of the mass of a Rb to Mo nucleus!) and short lifetime (0.26 yoctoseconds $= 0.26 \times 10^{-24}$ s).

This force is thus very weak and of very short range (<0.1 fm) and one might therefore think that, similar to the even weaker gravitational force (mediated by the still hypothetical graviton of spin 2), it should not contribute significantly to the forces between the particles in molecules (nuclei and electrons). Indeed, the weak force, because of its short range, becomes effective in molecules, when the electrons penetrate the nucleus, and then it leads only to a very small perturbation on the molecular dynamics, which ordinarily might be neglected completely.

It turns out, however, that because of the different symmetry groups of the electromagnetic and the electroweak Hamiltonians there arises a fundamentally important, new aspect in the dynamics of chiral molecules, which we therefore have added to the figure from CERN, where this was

not originally included, in our Figure 6.3. Indeed, the electromagnetic Hamiltonian commutes with the space inversion or parity operator $\hat{P}$

$$\hat{P}\hat{H} = \hat{H}\hat{P} \tag{6.2}$$

which leads to the consequence that in chiral molecules the delocalized energy eigenstates χ_+ and $-\chi_-$ have well-defined parity and the localized handed states λ and ρ of chiral molecules have exactly the same energy by symmetry (see Section 6.3 for details). Therefore one can also say that the reaction enthalpy $\Delta_R H_0^{\circ}$ for the stereomutation reaction (6.3) between R and S enantiomers of a chiral molecule would be exactly zero by symmetry ($\Delta_R H_0^{\circ} \equiv 0$) a fact originally noted already by van't Hoff[39]

$$\mathrm{R} \leftrightarrows \mathrm{S} \tag{6.3}$$

$$\Delta_R H_0^{\circ} = 0 \text{ (? Van't Hoff) or } \Delta_R H_0^{\circ} = N_A \Delta_{pv} E \text{ (today)}$$

Today, we know, that the electroweak Hamiltonian does not commute with $\hat{P}$

$$\hat{P}\hat{H}_{ew} \neq \hat{H}_{ew}\hat{P} \tag{6.4}$$

and therefore parity is violated leading to a small but non-zero parity-violating energy difference $\Delta_{pv}E$ between enantiomers and thus $\Delta_R H_0^{\circ} \neq 0$ (for example about 10^{-11} J mol^{-1} for a molecule like CHFClBr[40]). We shall discuss in Section 6.3, in more detail, under which circumstances such small effects lead to observable results dominating the quantum dynamics of chiral molecules.

This symmetry violation in chiral molecules is, indeed, the key concept that leads to an interesting interaction between high energy physics and molecular physics and chemistry; indeed also biochemistry.[36,41,42] It results in the following at first perhaps surprising three statements:

1. The fundamentally new physics arising from the discovery of parity violation[22–26] and the consequent electroweak theory in the standard model of particle physics (SMPP)[43–47] leads to the prediction of fundamental new effects in the dynamics of chiral molecules and thus in the realm of chemistry.
2. Molecular parity violation as encoded in eqn (6.2)–(6.4) has possibly (but not necessarily) important consequences for the evolution of biomolecular homochirality in the evolution of life.[28,29,31,32,41,42,48,140]
3. Possible experiments on molecular parity violation open a new window to looking at fundamental aspects of the standard model of high energy physics, and thus molecular physics might contribute to our understanding of the fundamental laws relevant to high energy physics. Indeed, going beyond parity violation and the standard model, molecular chirality may provide a new look at time-reversal symmetry and its violation, in fact the nature of time.[42,110,139,157,161]

It should thus be clear that electroweak quantum chemistry has interesting lessons to tell. A brief history of electroweak quantum chemistry is quickly told. After the discovery of parity violation in 1956/57[22–26] it took

about a decade until the possible consequences for chemistry and biology were pointed out by Yamagata in 1966.[48] While his numerical estimates were wrong by many orders of magnitude (as also was a later estimate[49]) and even some of his qualitative reasonings were flawed (see ref. 36), the link between parity violation in high energy physics and the molecular physics of chirality was thus established and repeatedly discussed qualitatively in the 1970s.[50–57]

The first quantitative calculations on molecular parity violation were carried out following the work of Hegström, Rein and Sandars[58,59] and Mason and Tranter[60–67] including several discussions by others in the 1980s.[68–82] Some far-reaching conclusions about consequences for biomolecular homochirality were drawn from some of these early calculations but we know now that none of these early calculations prior to 1995 can be relied on (nor can one retain their conclusions), as they were wrong by orders of magnitude.

Indeed, in 1995, we carefully reinvestigated the calculations of parity-violating energies in molecules and discovered, surprising to many at the time, that an improved theoretical treatment leads to an increase of calculated parity-violating energies by about two orders of magnitude in the benchmark molecules H_2O_2 and H_2S_2.[33–35] This discovery triggered substantial further theoretical[40–42,83–97] and proposals for experimental activity[98–109] and the numerical results were rather quickly confirmed in independent calculations from several research groups, as summarized in Table 6.1. Figure 6.4 provides a graphical survey of the development and Figure 6.5 shows the structures and coordinate definitions for HSSH. Both in Table 6.1 and Figure 6.4, one can see the ''big jump'' by about a

Table 6.1 Comparison of E_{pv} (in 10^{-20} E_h, with $\tau = 45^\circ$) and $\Delta_{pv}E^{el} = E_{pv}(M) - E_{pv}(P)$ (in 10^{-14} hc cm^{-1}, at $\tau = 90^\circ$) for the molecules HOOH and HSSH computed with various methods. Adapted from ref. 151 with permission from Taylor and Francis, Copyright 2015. See also ref. 29, 30, 36, 111 and 128, and Figure 6.5 for coordinate definitions (schematic). One notes the ''big jump'' of about a factor 100 occurring in 1995/96.

Method[a] (the year)	E_{pv}(HOOH)	$\Delta_{pv}E^{el}$(HOOH)	E_{pv}(HSSH)	$\Delta_{pv}E^{el}$(HSSH)
SDE-RHF[62] (1984)	−1.2	−0.03	−135.0	2.0
CIS-RHF[33,34,83,84,128] (1995/6)	−39.7	−5.0	−1654.0	188.1
TDA[86] (1997)	−55.9	−7.0	−1487.7	161.5[b]
CPHF[151] (2015)	−61.38	−2.9	−1865.6	242.0
MC-LR-RPA[35,83,85,128,153] (2000)	−60.88	−2.8	−1913.0	185.0
CASSCF-LR[35,85] (2000)	−45.00	−3.4		
CCSD[151] (2015)	−51.69	−6.4	−2248.6	238.3
ZORA-HF[155] (2005)	−79.30	−3.9	−2350.0	294.5
ZORA-B3LYP[125] (2005)	−65.40	−8.3	−2690.0	290.0
ZORA-BLYP[125] (2005)	−69.30	−9.9	−2750.0	278.3
DC-HF[88] (1999)	−70.60	−4.0	−2077.0	280.0
DC-MP2[154] (2005)	−57.88	−7.3	−2112.0	224.3
DC-CCSD(T)[156] (2000)	−61.20	−8.8	−2110.0	215.1

[a]Note the equivalence, in principle, of methods as given in the parentheses (CIS-RHF, CIS-LR, TDA) and (CPHF, RPA), differences arising only because of slight differences in numerical methods applied in the independent calculations by different authors. In ref. 151 $E_{pv}(P) - E_{pv}(M) = \Delta_{pv}E^{el}$ was given for H_2O_2 in order to give positive values (see ref. 151 and 159 for an explanation of acronyms).

[b]In principle the TDA value of ref. 86 should be scaled by 75% to give a value of 120× 10^{-14} hc cm^{-1}, see ref. 36 and 84.

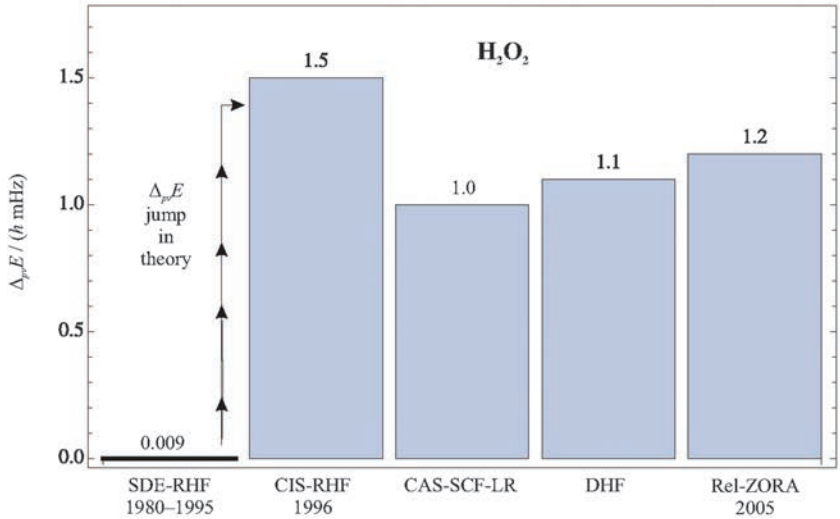

Figure 6.4 Graphical survey of the development of the theory of molecular parity violation with the "big jump" in 1995.
Reproduced from ref. 158 with permission from the Royal Society of Chemistry.

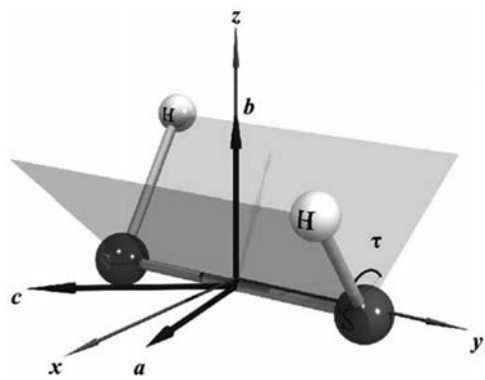

Figure 6.5 Equilibrium structure of HSSH (*P*-enantiomer) as obtained with the CCSD(T) method and cc-pV5Z basis set shown in the so-called electrostatic reference frame with axes (grey) labelled *x, y* and *z* together with the so-called molecular main chiral axes[84] *a, b* and *c* (black). The equilibrium structural parameters are $r_e(SS) = 207.64$ pm, $r_e(SH) = 134.32$ pm, $\alpha_e(SSH) = 98.0^\circ$, $\tau_e = 90.72^\circ$.
Adapted from ref. 128 with permission from John Wiley and Sons, © 2004 Wiley Periodicals, Inc., and from ref. 151 with permission from Taylor and Francis, Copyright 2015.

factor of 100 that occurred after 1995 compared to previous values and the consistency of high results afterwards (see also ref. 36 and 111 for some history). While the earlier overoptimistic conclusions on the selection of biomolecular homochirality had to be revised,[36] our work has led to a completely new and much more optimistic outlook on the possibility of doing successful

spectroscopic experiments, which are now underway in our own group and others, following several proposed schemes.[27,30,32,98–107,149,152,174–176,181,182] Although no successful experiment has as yet been reported, one may now expect such results in the relatively near future.

In his insightful and enlightening summaries of the status of quantum chemistry in the 1980s Henry F. Schaefer III noted the arrival of what was to be called the ''third age of quantum chemistry''.[112–114] This age was characterized by the new ability of theoretical quantum chemistry to provide accurate numerical results for chemically relevant species (such as CH_2[115,116]) that could either challenge or overturn apparently established experimental results or else also make reliable predictions for still unavailable but potentially important experimental results. These statements hold true even more today. However, this ''third age of quantum chemistry'' is entirely based on the Schrödinger–Dirac-like theory including only the electromagnetic force. We might call this ''electromagnetic quantum chemistry'' (the further development of accurate results for rovibrational energy levels called the ''fourth age'' also falls in this domain[117]).

In the 1990s, however we introduced the term ''electroweak quantum chemistry'',[33,34] to characterize a theory making quantitatively reliable predictions for phenomena related to fundamental dynamical properties of chiral molecules. In a sense this is a new age for physical stereochemistry. While the predictions appear to be stable and quantitatively reliable from a theoretical point of view, they are ''true predictions'', as so far there is no experimental result yet available (beyond null results consistent with theory). Thus this new electroweak quantum chemistry still awaits experimental test, and we shall return to this question.

6.2.2 Basic Theory

As we pointed out in the introduction, there was a dramatic change in our quantitative understanding of parity-violating potentials calculated from electroweak quantum chemistry from about 1995.[33,34] One starting point for this was our observation[33] that there were surprisingly large deviations of the older theoretical calculations from simple estimates following an equation proposed by Zel'dovich and coworkers[56]

$$\frac{\Delta_{\mathrm{pv}}E}{h} \cong 10^4 \frac{Z^5}{100^5}\,\mathrm{Hz}. \tag{6.5}$$

This by itself was not such a strong argument, given the complexity of the problem and the many possibilities for compensation of contributions leading to lower values of parity violation than expected from simple estimates. Indeed, we could rationalize such compensations by analysing the calculated parity-violating potentials in terms of a trace of a tensor[33,34] under certain conditions, thus

$$E_{\mathrm{pv}} = E_{\mathrm{pv}}^{XX} + E_{\mathrm{pv}}^{YY} + E_{\mathrm{pv}}^{ZZ}. \tag{6.6}$$

As the three components frequently differ in sign, this explains a certain lowering below the maximum possible values realized for the individual components. However, an even more important observation is related to the RHF wave functions used in the older calculation being really quite inappropriate. Indeed, the simplest improvement of using excited state CIS (configuration interaction singles) wave functions had already introduced an increase in parity-violating potentials by about two orders of magnitude,[33,34,84,85] a result later corroborated by our much improved MC-LR approach[35,85] and further confirmed independently by several other groups as well as in further calculations by our group[86–97] (see also ref. 36, 97 and 111 for some history).

We shall provide here a brief outline of the new theory following ref. 33, 34, 35, 84 and 85 in order to also provide a basic understanding of the limitations and omissions in current approaches (see also ref. 27 and 111 and further references cited therein).

In the framework of the standard model, the relevant parity-violating interaction is mediated by the electrically neutral Z^0 bosons. At molecular energies that are much lower than the energy (corresponding to mc^2) of the Z^0-boson (91.1876 GeV) the contribution of Z^0 becomes virtual.[118–120] This leads at low energies to the Hamiltonian density of the fully relativistic parity-violating electron–neutron interaction of the following form (with $h/2\pi \equiv c \equiv 1$, to simplify notation here, returning to SI units later).

$$\begin{aligned}\hat{H}^{(e-n)}(x) = \frac{G_F}{2\sqrt{2}} g_A (1 - 4\sin^2\Theta_w) j_\mu[\psi^{(el)}(x)] \\ \times j^\mu_{(ax)}[\psi^{(n)}(x)] + \frac{G_F}{2\sqrt{2}} j_\mu[\psi^{(n)}(x)] \\ \times j^\mu_{(ax)}[\psi^{(el)}(x)]\end{aligned} \tag{6.7}$$

with $j^\mu_{(ax)}[\psi(x)]$ involving the familiar γ-matrices[118,119]

$$j^\mu_{(ax)}[\psi(x)] \stackrel{\text{def}}{=:} \Psi^+(x)\gamma^0\gamma^\mu\gamma^5\Psi(x). \tag{6.8}$$

The γ^5 matrix converts the four-vector $j^\mu[\psi(x)]$ into the axial vector $j^\mu_{(ax)}[\psi(x)]$. Similar expressions are obtained for the electron–proton and the electron–electron interactions.[34,120]

In principle, as pointed out in ref. 34, one can use these relativistic equations as a starting point for the theory; relativistic theories of this type have been carried out at different levels of approximation for instance by the group of Barra, Robert and Wiesenfeld (Hückel-type)[68,69,72,73] and four-component relativistic theory by Schwerdtfeger and coworkers.[88,94,95] Omitting the two small components of the bispinors $\Psi^n(x)$ and $\Psi^{el}(x)$, and

thus converting from four component bispinors to two-component spinors following ref. 34, 120–122 one obtains ($\mathrm{i} = \sqrt{-1}$)

$$\hat{H}^{(\mathrm{e}-n)}(\boldsymbol{x}) = \frac{G_\mathrm{F}}{4\sqrt{2}\mu c}[-\psi^{\dagger(n)}(\boldsymbol{x})\psi^{(n)}(\boldsymbol{x})\{\psi^{\dagger(\mathrm{el})}(\boldsymbol{x})\boldsymbol{\sigma}(\boldsymbol{P}\psi^{(\mathrm{el})}(\boldsymbol{x})) + (\boldsymbol{P}^{\star}\psi^{\dagger(\mathrm{el})}(\boldsymbol{x}))\boldsymbol{\sigma}\psi^{(\mathrm{el})}(\boldsymbol{x})\} + \mathrm{i}g_\mathrm{A}(1 - 4\sin^2\Theta_\mathrm{w})\boldsymbol{P}(\psi^{\dagger(\mathrm{el})}(\boldsymbol{x})\boldsymbol{\sigma}\psi^{(\mathrm{el})}(\boldsymbol{x})\psi^{\dagger(n)}(x))\boldsymbol{\sigma}\psi^{(n)}(\boldsymbol{x})] \tag{6.9}$$

G_F is the Fermi constant,[147,159] $\boldsymbol{P}$ the momentum operator, $\boldsymbol{\sigma}$ the doubled spin operator that has as components the familiar 2×2 Pauli matrices, $\boldsymbol{x}$ the spatial coordinate set and μ the reduced mass of the electron. The last term in eqn (6.9) is taken to be small because of the extra prefactor $(1 - 4\ \sin^2\ \Theta_\mathrm{w}) \simeq 0.0724$ (depending on the scheme used for the Weinberg parameter[151] and possibly energy dependent) and because of the dependence on neutron (and similarly proton) spin with the tendency of spin compensation in nuclei. The form factor g_A (from the strong interaction of the neutron) can be taken as 1.25.[34]

Finally, replacing the neutron density by a delta function because of the contact-like nature of the very short-range weak interaction

$$\Psi^{\dagger(n)}(\boldsymbol{x})\Psi^{(n)}(\boldsymbol{x}) \cong \delta^3\ (\boldsymbol{x} - \boldsymbol{x}^{(n)}) \tag{6.10}$$

one obtains a Hamilton operator for the electron–neutron interaction

$$\hat{H}^{(\mathrm{e}-n)} = -\frac{G_\mathrm{F}}{4\mu c\sqrt{2}}(\boldsymbol{P}\boldsymbol{\sigma}\delta^3(\boldsymbol{x} - \boldsymbol{x}^n) + \delta^3(\boldsymbol{x} - \boldsymbol{x}^n)\boldsymbol{P}\boldsymbol{\sigma}). \tag{6.11}$$

For the electron–proton interaction the Hamiltonian is similarly

$$\hat{H}^{(\mathrm{e-p})} = -\frac{G_\mathrm{F}}{4\mu c\sqrt{2}}(1 - 4\sin^2\Theta_\mathrm{W}) \cdot (\boldsymbol{P}\boldsymbol{\sigma}\delta^3(\boldsymbol{x} - \boldsymbol{x}^{(\mathrm{p})}) + \delta^3(\boldsymbol{x} - \boldsymbol{x}^{(\mathrm{p})})\boldsymbol{P}\boldsymbol{\sigma}). \tag{6.12}$$

Collecting the terms for neutrons and protons together and defining an electroweak charge Q_a of the nucleus a with charge number Z_a and neutron number N_a

$$Q_a = Z_a\ (1 - 4\ \sin^2\ \Theta_\mathrm{w}) - N_a \tag{6.13}$$

one gets an effective electron–nucleus interaction

$$\hat{H}_a^{(\mathrm{e-nucleus})} = -\frac{G_\mathrm{F}}{4\mu c\sqrt{2}}Q_a(\boldsymbol{P}\boldsymbol{\sigma}\boldsymbol{\delta}^3(\boldsymbol{x} - \boldsymbol{x}^{(\mathrm{nucleus})}) + \boldsymbol{\delta}^3(\boldsymbol{x} - \boldsymbol{x}^{(\mathrm{nucleus})})\boldsymbol{P}\boldsymbol{\sigma}). \tag{6.14}$$

In addition to the electron–nucleus interaction, one should consider the electron–electron interaction.

$$\hat{H}^{(\mathrm{e-e})} = \frac{G_\mathrm{F}}{2\mu c\sqrt{2}}(1 - 4\sin^2\Theta_\mathrm{W}) \cdot \left\{\delta^3(\boldsymbol{x}^{(1)} - \boldsymbol{x}^{(2)}), (\boldsymbol{\sigma}^{(1)} - \boldsymbol{\sigma}^{(2)}) \cdot (\boldsymbol{P}^{(1)} - \boldsymbol{P}^{(2)})\right\}_+ + \mathrm{i}[\delta^3(\boldsymbol{x}^{(1)} - \boldsymbol{x}^{(2)}), (\boldsymbol{\sigma}^{(1)} \times \boldsymbol{\sigma}^{(2)}) \cdot (\boldsymbol{P}^{(1)} - \boldsymbol{P}^{(2)})]_- \tag{6.15}$$

with obvious notation for the two electrons 1 and 2 in a pair $\{,\}_+$ for the anticommutator and $[,]_-$ for the commutator, used here for brevity.

The electron–electron contribution to the effective parity-violating potential is considered to be small,[34] below 1% of the other contributions, because of the small prefactor and the lack of a corresponding enhancement with Q_a and also because of a compensation of terms from different electron–electron pairs. Thus this term is usually neglected, although one must remember that it really consists of a sum over many electron pairs. Assembling all terms together and introducing the electron spin $\hat{\boldsymbol{s}}$ (with dimension) together with linear momentum $\hat{\boldsymbol{p}}$, the electron mass m_e, and rewriting now everything in consistent SI units throughout, one obtains finally for the electron–nucleus part of the Hamiltonian, using the common symbols and values for the fundamental constants[159]

$$\hat{H}_{\mathrm{pv1}}^{(\mathrm{e-nucl})} = \frac{\pi G_\mathrm{F}}{m_\mathrm{e} hc\sqrt{2}} \sum_{i=1}^{n}\sum_{a=1}^{N} Q_a\{\hat{\boldsymbol{s}}_i\hat{\boldsymbol{p}}_i\delta^3(\vec{r}_i - \vec{r}_a) + \delta^3(\vec{r}_i - \vec{r}_a)\hat{\boldsymbol{s}}_i\hat{\boldsymbol{p}}_i\}. \tag{6.16}$$

We empasize the very small value of the Fermi coupling constant $G_F = 1.43585\times10^{-62}$ Jm^3 in SI units. The sums extend over n electrons and N nuclei. This operator can be evaluated in different ways. The simple perturbative sum over states expression in the Breit Pauli approximation for the spin–orbit interaction reads for the parity-violating potential (with $\hat{H}_{\mathrm{pv}}^{\mathrm{e-nucleus}} \cong \hat{H}_{\mathrm{pvl}}^{\mathrm{e-nucl}}$)

$$E_\mathrm{pv} = 2\mathrm{Re}\left\{\sum_n \frac{\langle\psi_0|\hat{H}_{\mathrm{pv}}^{\mathrm{e-nucleus}}|\psi_n\rangle\langle\psi_n|\hat{H}_\mathrm{SO}|\psi_0\rangle}{E_0 - E_n}\right\}. \tag{6.17}$$

The Breit Pauli spin–orbit Hamiltonian $\hat{H}_\mathrm{SO}$ is as usual, here in SI units[151,159]

$$\hat{H}_\mathrm{SO} = \frac{e^2h^2\mu_0}{32\pi^3 m_e^2}\left[\sum_{i=1}^{n}\sum_{a=1}^{N} Z_a\frac{\hat{l}_{i,a}\hat{s}_i}{|\vec{r}_a - \vec{r}_i|^3} - \sum_{i=1}^{n}\sum_{j\neq i}^{n}\frac{\hat{l}_{i,j}(\hat{s}_i + 2\hat{s}_j)}{|\vec{r}_i - \vec{r}_j|^3}\right] \tag{6.18}$$

where $\hat{l}_{i,k}$ refers to the orbital angular momentum of electron i with respect to particle number k.

The sum-over-states expression [eqn (6.17)] essentially mixes the electronic ground-state singlet function with excited-state triplets in order to obtain a parity-violating energy expectation value for the true (mixed singlet-triplet) ground state (for a pure singlet this would vanish). However, the sum

over states expression, eqn (6.17), when used explicitly, converges slowly for larger molecules. It is well known in the framework of propagator methods[123,124] that the expression in eqn (6.17) is equivalent to the expression from response theory in eqn (6.19)[35,85]

$$E_{\mathrm{pv}} = \langle\langle \hat{H}_{\mathrm{pv}}; \hat{H}_{\mathrm{SO}} \rangle\rangle_{\omega=0} = \langle\langle \hat{H}_{\mathrm{SO}}; \hat{H}_{\mathrm{pv}} \rangle\rangle_{\omega=0}. \tag{6.19}$$

One can say that the parity-violating potential E_{pv} is the response of $\langle\psi_0|\hat{H}_{\mathrm{pv}}|\psi_0\rangle$ to the static ($\omega = 0$) perturbation $\hat{H}_{\mathrm{SO}}$ or *vice versa*. This multiconfiguration linear response approach (MCLR) was derived in ref. 35 and 85, to which we refer for details. It shows much better convergence properties than when evaluating eqn (6.17) directly.

We have given this brief summary of the theory developed in more detail in ref. 33–35 in order to show all the steps of the many successive approximations made. Each of these approximations can be removed when the necessity arises. For instance, if one wishes to describe explicitly hyperfine structure components or NMR experiments one must not neglect the spin-dependent terms and therefore one has to add to the operator of eqn (6.16) a further operator given by eqn (6.20)[35,85], using again anticommutator $\{,\}_+$ and commutator $[,]_-$:

$$\begin{aligned}\hat{H}_{\mathrm{pv2}}^{(\mathrm{e-nucl})} = \frac{\pi G_{\mathrm{F}}}{m_{\mathrm{e}} hc\sqrt{2}} \sum_{i=1}^{n} \Bigg[\sum_{a=1}^{N} (-\lambda_a)(1 - 4\sin^2\theta_{\mathrm{W}}) \{\hat{\boldsymbol{p}}_i \hat{\boldsymbol{I}}_{\boldsymbol{a}}, \delta^3(\vec{r}_i - \vec{r}_a)\}_+ \\ + (2\mathrm{i}\lambda_a)(1 - 4\sin^2\theta_{\mathrm{W}})(\hat{\boldsymbol{s}}_{\boldsymbol{i}} \times \hat{\boldsymbol{I}}_{\boldsymbol{a}})[\hat{\boldsymbol{p}}_i, \delta^3(\vec{r}_i - \vec{r}_a)]_- \Bigg].\end{aligned} \tag{6.20}$$

Also, sometimes the approximate ''theoretical'' value of the Weinberg parameter $\sin^2\,\Theta_{\mathrm{W}} = 0.25$ is taken, which simplifies the expressions with $(1 - 4\,\sin^2\,\Theta_{\mathrm{W}}) = 0.0$. However, more generally, the accurate experimental parameter will be used with $(1 - 4\,\sin^2\,\Theta_{\mathrm{W}}) = 0.0724$[34,159] which may further depend on the energy range considered. Furthermore, one might use the semirelativistic expressions using the Breit Pauli spin–orbit operator (6.18) and the operators for parity violation in eqn (6.16) and (6.20). This should be an excellent approximation for nuclei with maximum charge number $Z_a = 20$ and acceptable up to $Z_a = 40$. However, for more highly charged nuclei one must return to the relativistic eqn(6.7) and from there derive various approximate relativistic expressions, for instance in the four-component Dirac Fock framework[88] or within two-component relativistic approximations.[125] On the other hand, one might also use more approximate treatments such as density functional theory.[96,111,126]

One might also consider investigating explicit ''non-virtual'' couplings going beyond the use of eqn (6.7) as a starting point, or one might include the electron–electron parity-violating interaction in eqn (6.15) in the calculations. Whether one wishes to invest effort in removing some of the approximations used depends upon one's intuition of whether large improvements are to be expected. At present it seems unlikely that order of

magnitude improvements will again be found in the future, although only experiment can give a definitive answer. We think that the currently largest chance for improvement resides in appropriate electronic wave functions that are highly accurate, in particular near the nuclei, and in further effects from molecular structure and motion to be discussed now.

6.2.3 Parity-violating Potential Hypersurfaces and Vibrational Effects

Two qualitative aspects of the structure of parity-violating potentials deserve mentioning. Firstly, similar to the parity conserving electronic potential, the parity-violating potentials are a function of all 3N-6 internal nuclear degrees of freedom in the molecule. Thus, the parity-violating potentials E_{pv} defined by eqn (6.17) or (6.19) define a parity-violating potential hypersurface

$$E_{pv} = V_{pv}\,(q_1,\, q_2,\, q_3,\, \ldots\, q_{3N-6}). \tag{6.21}$$

While isolated distortions or individual coordinate displacements have been considered for some time in such calculations (see Figure 6.6 for instance) the true multidimensional aspects have been considered only more recently.[40,91,97,127,128] The spectroscopically observable parity-violating energy differences $\Delta_{pv}E$ have to be computed as appropriate expectation values of the parity-violating potential in eqn (6.21) for the multidimensional rovibrational state with anharmonically coupled vibrations. This leads to sizeable effects, as was shown recently.[127] However, we know from our work in rovibrational spectroscopy and dynamics of polyatomic molecules[129] that this problem can be handled accurately for not too complex molecules[98–100,129–133,172] and a similar statement applies to the other important dynamical problem: tunnelling (Section 6.3).

A second general aspect of the parity-violating potential arises from the structure of the Hamiltonian in eqn (6.16). Because of the contact-like interaction between electrons and nuclei, the parity-violating potential can be written as a sum of contributions from the individual nuclei

$$V_{pv}(q_1, q_2, q_3, \ldots\, q_{3N-6}) = \sum_{n=1}^{N} V_{pv}^{a}(q_1, q_2, q_3, \ldots\, q_{3N-6}). \tag{6.22}$$

Because of the approximate Z^5 scaling (see, however, ref. 128) this allows for an easy analysis of calculations and also some rough estimates. Because the electronic wave function generally depends upon the coordinates ($q_1, q_2, q_3, \ldots$ q_{3N-6}) in a very complex fashion, there are, however, no really simple and generally accurate estimates to be expected. However, one can derive certain sets of rules for special cases (see ref. 134 for example). In practice, one has to combine the traditional quantum chemical calculations from the ''electromagnetic theory'' with the parity-violating potentials from the electroweak theory, as we shall discuss now with emphasis on the symmetry aspects.

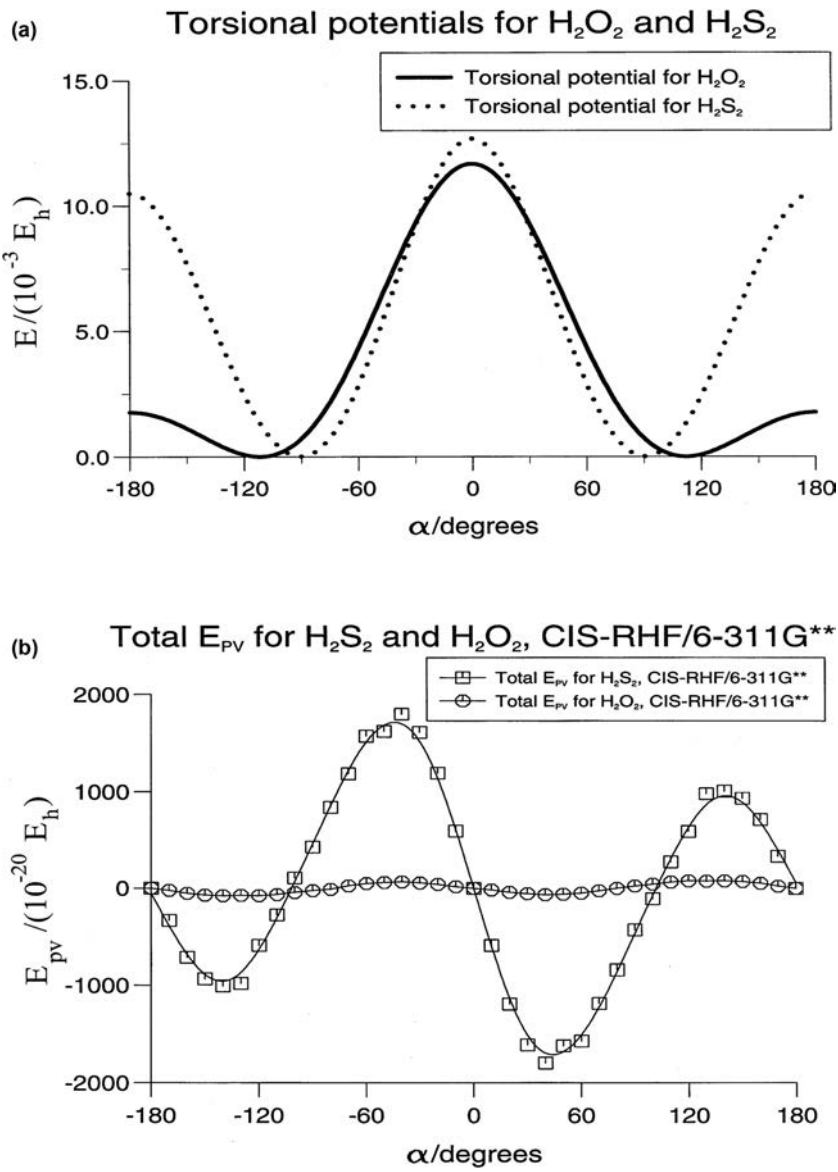

Figure 6.6 Parity conserving and parity-violating potentials for H_2O_2 (a) and H_2S_2 (b). Reproduced from ref. 84 with permission from Elsevier, Copyright 1998.

For visualization as well as for the practical approach on can use as a starting point the Born–Oppenheimer (or adiabatic) potential hypersurface $V(q_1, q_2, \ldots q_s)$ as a function of the set of some generalized internal coordinates $\{q_1, q_2, q_3 \ldots q_s\}$, where $s = 3N - 6$ is the relevant number of degrees of freedom of a chiral molecule with $N \geq 4$ being the number of nuclei (atoms) of the molecule. This potential is rigorously symmetric

upon inversion of the coordinates at the center of mass (parity operation $\hat{P}$ or $\hat{E}^*$)

$$E^* V_R(q_1, q_2, q_2, \ldots q_s) = V_S(\bar{q}_1, \bar{q}_2, \bar{q}_3, \ldots \bar{q}_s) \tag{6.23}$$

with

$$V_R(q_1, q_2, q_2, \ldots q_s) - V_S(\bar{q}_1, \bar{q}_2, \bar{q}_3, \ldots \bar{q}_s) = 0 \tag{6.24}$$

i.e. exactly zero by symmetry. We have indicated by the indices R and S that the inversion E^* transforms an enantiomeric configuration ''R'' into the corresponding enantiomeric ''S'' configuration, and the $\bar{q}_i$ indicate the coordinates with the inverted structure.

Of course, the symmetry of the Hamiltonian goes far beyond the Born–Oppenheimer, adiabatic or any other approximation; the exact molecular Hamiltonian $\hat{H}_{em}$ in electromagnetic theory shows this symmetry. One notes that relevant molecular quantizations and potential energy differences in these potentials are on the order of 100 kJ mol^{-1} corresponding to about 1 eV (covering of course a range of a few orders of magnitude depending on the dynamical process considered).

On the other hand, in electroweak quantum chemistry, one calculates an additional effective ''parity-violating'' potential $V_{pv}(q_1, q_2, q_2, \ldots q_s)$, which is antisymmetric under the inversion operation.

$$E^* V_{pvR}(q_1, q_2, q_2, \ldots q_s) = V_{pvS}(\bar{q}_1, \bar{q}_2, \bar{q}_3, \ldots \bar{q}_s) = -V_{pvR}(q_1, q_2, q_2, \ldots q_s) \tag{6.25}$$

Thus one can define for every structure of the chiral molecule a parity-violating energy difference

$$\begin{aligned} \Delta_{pv}E_{el}(q_1, q_2, q_3, \ldots q_s) &= V_{pvR}(q_1, q_2, q_3, \ldots q_s) - V_{pvS}(\bar{q}_1, \bar{q}_2, \bar{q}_3, \ldots \bar{q}_s) \\ &= 2V_{pvR}(q_1, q_2, q_3, \ldots q_s). \end{aligned} \tag{6.26}$$

These energy differences are typically very small in absolute value, on the order of 100 aeV or 10^{-11} J mol^{-1} and can be negative or positive depending whether R or S is more stable. They vanish by symmetry for achiral geometries of the molecule. For chiral geometries they satisfy the antisymmetry relation in eqn (6.25). However, even within one set of enantiomeric geometries (say only for the R-isomer) the parity-violating potentials can change sign. Thus there can be, and, indeed, there frequently are, vanishing parity-violating potentials (and $\Delta_{pv}E_{el}$) also for *chiral* geometries (see Figure 6.6). This property can be understood by the interpretation of the structure of the parity-violating potential as a trace of a tensor, thus the sum of three components of possibly different signs, but it does not depend on this interpretation.[33,34,84] While well understood, this property spoils any simplistic approach to estimate measurable parity-violating energy differences from theory. They can only be obtained from appropriate theoretical calculation of the parity-violating potential energy hypersurfaces in eqn (6.25) and (6.26) for the relevant set of geometries. Although one can give some simple rules for estimating orders of magnitude of parity-violating

potentials, such as the approximate Z^5 scaling with nuclear charge[27,30,33–35,84,85,158] large deviations can occur for individual molecules, for instance if the V_{pv} crosses zero near the chiral equilibrium geometry of the molecule. The chiral molecule 1,3-difluoroallene is such an example.[141,151] Another example is the amino acid alanine, where one has a zero crossing of V_{pv} as a function of a conformational change that is unrelated to enantiomeric structure.[34,92] Thus the actual calculation of the parity-violating potentials by the methods of quantitative electroweak quantum chemistry is necessary, if one wants to obtain accurate results. We do not discuss details here but refer to careful descriptions[27,33–35,40,84,85,88,91–93,96,97,127,128,141–146,151] as an incomplete survey of recent work of this kind.

The parity-violating potentials or parity-violating energy differences $\Delta_{pv}E_{el}$ in eqn (6.25) and (6.26) do not correspond to the directly measurable parity-violating energy difference $\Delta_{pv}E$, for instance in the ground state energy difference between the R and S enantiomers. This is calculated as an expectation value over $\Delta_{pv}E_{el}$ in the ground rotational-vibrational (perhaps also hyperfine) state. Thus in practice one uses

$$\hat{H} = \hat{T} + \hat{V}_R(q_1, q_2, q_2, \ldots q_s) \tag{6.27}$$

obtaining ideally

$$\hat{H}\varphi_{evr}^{(k)} = E_{evr}^{(k)}\,\varphi_{evr}^{(k)} \tag{6.28}$$

by solving for the complete rovibronic wave functions $\varphi_{evr}^{(k)}(q_1, q_2, q_3, \ldots q_s)$ of the electronic ground or some excited state, and if needed including non-adiabatic and hyperfine structural effects. One obtains the desired parity-violating energy differences as expectation values

$$\Delta_{pv}E^{(k)} = \langle \varphi_{evr}^{(k)} | \Delta_{pv}E_{el} | \varphi_{evr}^{(k)} \rangle. \tag{6.29}$$

The index "evr" for the internal quantum state of the molecule is considered to include the nuclear spin (hyperfine structure) wave function in molecules possessing nuclei with non-zero spin and in this case the parity-violating Hamiltonian $\hat{H}_{pv}$ to calculate E_{pv} in eqn (6.17) should include the term $\hat{H}_{pv1}$ in eqn (6.16) and also the term $\hat{H}_{pv2}$ from eqn (6.20). Calculations of this type have been presented at various levels of approximation in ref. 40 and 127, for instance. For the rovibrational ground state ($k = 0$) we simply use the symbol $\Delta_{pv}E$ and for some excited states we use $\Delta_{pv}E^*$. As a first approximation, one frequently takes $\Delta_{pv}E_{el}$ at the equilibrium geometry $(q_1^e, q_2^e, q_3^e, \ldots q_s^e)$ in order to estimate $\Delta_{pv}E$ in the ground state. We have shown, however, that the effects from calculating the correct average by means of eqn (6.29) can be quite large.[127]

We can summarize the theoretical calculation of the parity-violating effects in chiral molecules by stressing again the symmetry aspect. While there is, of course, no current or in the foreseeable future possible technology to calculate quantum chemical energies (say $V_R(q_1, q_2, q_3, \ldots q_s)$ in eqn (6.23) or rovibrational and hyperfine levels, *etc.*) to an accuracy of, say, 100 aeV, which is the order of the electroweak effects, such an accuracy is not needed, because we know that the difference in eqn (6.24) and all similar energy

differences derived from ''electromagnetic'' quantum chemistry are exactly zero by symmetry (beyond the Born–Oppenheimer approximation and even including effects from electromagnetic quantum field theory). Thus parity-violating energy differences can be calculated separately and accurately as purely antisymmetric contribution to the effective potentials or level energies, in spite of their extremely small absolute magnitude. In the well-known ''captain and ship'' analogy we can say that we can obtain the weight of the captain alone separately and we do not have to weigh the ship with the captain and then the ship alone and calculate the difference between the two results, which would be impossible in terms of significant accuracy; this direct evaluation of the ''weight of the captain'', corresponding to the parity-violating potential is made possible by symmetry. A similar statement holds for experiments on the effect, to be discussed in Section 6.5 (see also the discussion in ref. 27, 28 and 30).

6.3 The Interplay of Tunnelling and Parity Violation in Chiral Molecules

Having now the ability to calculate accurately and quantitatively the effective parity-violating potentials from electroweak quantum chemistry we can discuss the effects on the quantum dynamics of chiral molecules in relation to tunnelling according to Hund's ''electromagnetic theory''. This is summarized schematically in Figure 6.7, which compares the theoretical situation at the time of Hund, as discussed in the introduction, with the current situation including parity violation in a simple one-dimensional picture of the effective potentials as a function of q.

The one-dimensional ''reaction coordinate'' q relates the two enantiomers and we keep the true multidimensional nature in mind. For reasons of symmetry the eigenstates in the electromagnetic theory will have a well-defined parity and are delocalized. They differ by a tunnelling splitting $\Delta E_{\pm} = E_{-} - E_{+}$ which might be very small. The delocalized eigenstates χ_{+} and $-\chi_{-}$ can be combined to give localized, time-dependent states λ and ρ as discussed in the introduction. We can use χ_{+} and $-\chi_{-}$ also as basis states when introducing the effects from parity violation as a small perturbation. For simplicity, we assume here that both $\Delta E_{\pm}$ and $\Delta_{\mathrm{pv}}E(q_1, q_2, q_3, \ldots q_s)$ are small compared to all the other energy differences between, say, rovibrational levels of the molecule. This allows us to treat the perturbation as a two-level problem, but the treatment can be readily extended to other situations by including more levels. We can distinguish now two limiting situations. In the first case we have

$$|\Delta E_{\pm}| \gg |\Delta_{\mathrm{pv}}E(q_1, \ldots\ldots q_s)|. \tag{6.30}$$

In this limiting case the perturbation will lead only to very small shifts in the energy levels, which remain almost unchanged, as will the tunnelling times in eqn (6.1). The perturbation also leads small ''parity-violating'' admixtures of the opposite parity in the wave functions, whose overall shape will, however, be

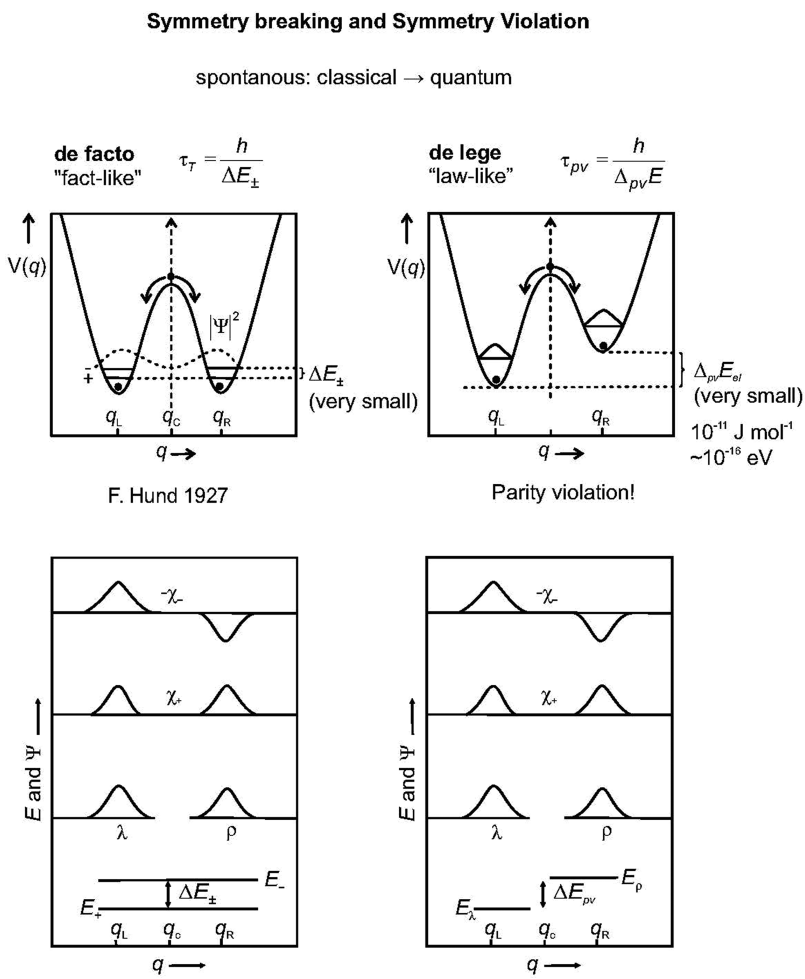

Figure 6.7 Illustration of symmetric and asymmetric double-well potentials for a chiral molecule.
Reproduced from ref. 30 with permission from the Annual Review of Physical Chemistry, Copyright 2008 (see also ref. 149).

essentially unchanged. Thus, in this case the time-dependent eigenstate dynamics and the time-dependent wave packet dynamics will be almost unchanged. This situation applies to transiently chiral molecules to be discussed below. A similar situation applies also to achiral molecules with eigenstates of well-defined parity. The effect of parity violation might still become visible by tiny effects such as changes in the optical selection rules, and a very small optical activity. However, these effects will not be dramatic and not be easily detected. In the other limiting case we have

$$|\Delta_{\mathrm{pv}}E(q_1, \ldots\ldots q_s)| \gg |\Delta E_\pm|. \tag{6.31}$$

This situation applies to stable chiral molecules where $\Delta E_\pm$ can be exceedingly small. In this case one observes a dramatic change. The eigenstates become

localized left or right (λ and ρ), that is, the stereomutation times become infinite. While one might say that a change from slow stereomutation tunnelling in, say, a million years to infinite (no tunnelling) is practically irrelevant and not observable in real experiments, there is a second change that is really observable. While in electromagnetic theory the lifetime of the parity eigenstates χ_+ and χ_- are infinite, in electroweak theory the parity eigenstates become in this limit time dependent, evolving with a period

$$\tau_{\mathrm{pv}} = h/\Delta_{\mathrm{pv}}E \tag{6.32}$$

where $\Delta_{\mathrm{pv}}E$ is the energy separation of the energy eigenstates λ and ρ. Within this limit one has also

$$\chi_+ = \frac{1}{\sqrt{2}}(\lambda + \rho) \tag{6.33}$$

$$-\chi_- = \frac{1}{\sqrt{2}}(\lambda - \rho) \tag{6.34}$$

and similarly

$$\lambda = \frac{1}{\sqrt{2}}(\chi_+ - \chi_-) \tag{6.35}$$

$$\rho = \frac{1}{\sqrt{2}}(\chi_+ + \chi_-) \tag{6.36}$$

(see also Figure 6.7). While the superposition principle guarantees that parity eigenstates χ_+ and χ_-can be prepared by superposition of λ and ρ, it turns out that theoretical values of $\Delta_{\mathrm{pv}}E$ such that periods for parity changes happen on a timescale of seconds, which is readily accessible to laboratory experiments.

Some further aspects of the time dependence in the two limits may be useful. The time-dependent Schrödinger equation for the wave function $\Psi(q, t)$ for the isolated molecule with the Hamiltonian $\hat{H}$ is:

$$\mathrm{i}\frac{h}{2\pi}\frac{\partial\Psi(q,t)}{\partial t} = \hat{H}\Psi(q,t) \tag{6.37}$$

with the general solution in terms of eigenfunctions φ_k and energies E_k

$$\hat{H}_k\varphi_k(q) = E_k\varphi_k(q) \tag{6.38}$$

$$\Psi(q,t) = \sum_k c_k\varphi_k \exp(-2\pi\mathrm{i}E_k t/h). \tag{6.39}$$

In the limit of eqn (6.30), where the eigenstates are to an excellent approximation given by χ_+ and χ_-, with energies E_+ and E_-, one thus has for the two-level evolution

$$\Psi(q,t) = \frac{1}{\sqrt{2}}\exp(-2\pi i E_+ t/h)[\chi_+ + \chi_- \exp(-2\pi i \Delta E_\pm t/h)] \tag{6.40}$$

with a probability density

$$P(q,t) = \Psi(q,t)\Psi^*(q,t) = |\Psi|^2 = \frac{1}{2}\left|[\chi_+ + \chi_- \exp(-2\pi i \Delta E_\pm t/h)]\right|^2 \tag{6.41}$$

This describes a structural change of the molecule from left to right during a tunnelling stereomutation.

In the opposite limit of eqn (6.31), where parity violation dominates, the eigenstates φ_k are given by λ and ρ with eigenvalues E_λ and E_ρ to an excellent approximation, and one has for the time-dependent wave function

$$\psi(q,t) = \frac{1}{\sqrt{2}}\exp(-2\pi i E_\lambda t/h)[\lambda + \rho \exp(-2\pi i \Delta_{pv} E t/h)]. \tag{6.42}$$

Now one can follow a change of the parity of the state (or wave function) with time. For $t = 0$ in eqn (6.42) one has a state χ_+ of positive parity, eqn (6.33), the probability of finding positive parity is 1 and the probability of finding negative parity is zero. However with increasing time one finds for the state of negative parity the probability

$$p_- = 1 - p_+ = \sin^2(\pi t \Delta_{pv} E/h). \tag{6.43}$$

From this discussion, it is clear that, for a significant assessment of parity violation in chiral molecules, one has to discuss the role of both parity violation and tunnelling. Only in the limit, where parity violation dominates [eqn (6.31)], will $\Delta_{pv}E$ be a measurable parity-violating energy difference between the ground-state energies of the localized enantiomers of chiral molecules. In the opposite limit of eqn (6.30), one would simply measure a tunnelling splitting between achiral states of rather well-defined parity. Table 6.2 gives a survey of results for $|\Delta_{pv}E^{el}|$ and $|\Delta E_\pm|$ for many molecules, from which the relevant times can be readily calculated as well. Table 6.3 summarizes theoretical results for parity violation in chiral molecules, where the tunnelling splitting is extremely small but has not been calculated quantitatively. However, in any case for all these molecules in Table 6.3 one has the limiting behavior $|\Delta_{pv}E| \gg |E_\pm|$ corresponding to eqn (6.31) with absolute certainty, whereas for the examples calculated in Table 6.2 this limit applies only to the six molecules ClOOCl, ClSSCl, D_2Te_2, T_2Te_2, HSSSH, and $C_4H_4S_2$. We note here also that the relative differences between $\Delta_{pv}E^{el}$ and $\Delta_{pv}E_0$ (*i.e.* averaged over the vibration-rotation ground-state wave function) are particularly large for molecules that are chiral by isotopic substitution of hydrogen isotopes H, D, and T (see ref. 134 for a discussion).

Table 6.2 Tuning tunnelling and parity violation in a series of molecules (modified and updated after ref. 29, 30 and 135).

Molecule	$\lvert\Delta E_{pv}^{el}\rvert/cm^{-1}$	$\lvert\Delta E_{\pm}\rvert/cm^{-1}$	Reference
H_2O_2	4×10^{-14}	11	35, 85, 131, 132, 137
D_2O_2	4×10^{-14}	2	35, 85,132
T_2O_2	4×10^{-14}	0.5	138
HSOH	4×10^{-13}	2×10^{-3}	138
DSOD	4×10^{-13}	1×10^{-5}	138
TSOT	4×10^{-13}	3×10^{-7}	138
$HClOH^+$	8×10^{-13}	2×10^{-2}	135
$DClOD^+$	$(8\times10^{-13})^c$	2×10^{-4}	135
$TClOT^+$	$(8\times10^{-13})^c$	7×10^{-6}	135
H_2S_2	1×10^{-12}	2×10^{-6}	89
D_2S_2	1×10^{-12}	5×10^{-10}	89
T_2S_2	1×10^{-12}	1×10^{-12}	89
Cl_2O_2	5.75×10^{-13}	6.7×10^{-25}	150–152
Cl_2S_2	1×10^{-12}	$\approx10^{-76}$[a]	90
H_2Se_2	2×10^{-10}[d]	1×10^{-6}	173
D_2Se_2	$(2\times10^{-10})^c$	3×10^{-10}	173
T_2Se_2	$(2\times10^{-10})^c$	4×10^{-13}	173
H_2Te_2	3×10^{-9}[b]	3×10^{-8}	135
D_2Te_2	$(3\times10^{-9})^c$	1×10^{-12}	135
T_2Te_2	$(3\times10^{-9})^c$	3×10^{-16}	135
HSSSH	1.61×10^{-12}	3.3×10^{-23}	164, 165
$C_4H_4S_2$	1.1×10^{-11}	$<1\times10^{-24}$	162, 166

[a] Extrapolated value.
[b] Calculated in ref. 88 for the P-structure ($r_{TeTe}=284$ pm, $r_{HTe}=164$ pm, $\alpha_{HTeTe}=92^\circ$ and $\tau_{HTeTeH}=90^\circ$) and the corresponding M-structure. An earlier, very approximate result by Wiesenfeld[73] should be cited as well, giving $\Delta E_{pv}=8\times10^{-10}\,cm^{-1}$ for the following structure ($r_{TeTe}=271.2$ pm, $r_{HTe}=165.8$ pm, $\alpha_{HTeTe}=90^\circ$ and $\tau_{HTeTeH}=90^\circ$).
[c] Not calculated quantitatively, but estimated to be rather similar to the corresponding hydrogen isotopomers.
[d] Calculated in ref. 88 for the P-structure ($r_{HSe}=145$ pm, $\alpha_{HSeSe}=92^\circ$ and $\tau_{HSeSeH}=90^\circ$) and the corresponding M-structure.

Figure 6.8 provides a graphical survey for the transition between the regimes of dominating tunnelling and dominating parity violation, where one can also identify the very approximate "Z^5 scaling law" for a series of hydrides of the chalcogenes[158] (see also ref. 128 for a discussion of the origin and limitations of the scaling law).

Some of the results summarized in Table 6.3 deserve further discussion. The relatively small absolute value of the parity-violating energy difference $\Delta_{pv}E^{el}$ at the equilibrium geometry (and also in the ground state) for 1,3-difluoroallene CHF=C=CHF arises because of a transition from positive to negative values of the parity-violating potential $\Delta_{pv}E^{el}(\alpha)$ as function of the torsional angle α at a chiral geometry rather near to the equilibrium geometry. The maximum of $\Delta_{pv}E^{el}(\alpha)$ would be more than an order of magnitude larger. This type of behaviour is rather frequent and is one of the reasons why simple empirical rules and scaling laws are not sufficient for an accurate estimate of $\Delta_{pv}E$ in the ground states of chiral molecules. On the other hand the relatively large value of $\Delta_{pv}E$ for 1,2-dithiine ($C_4H_4S_2$) in

Table 6.3 Parity-violating energy differences $\Delta_{pv}E$ between the ground states (and taken to be sometimes approximately $\Delta_{pv}E^{el}$ at the equilibrium structures) of chiral molecules, for which the tunnelling splitting is extremely small (but not quantitatively calculated, as one has certainly $|\Delta E_{\pm}| \ll |\Delta_{pv}E|$).

Molecule	$\lvert\Delta_{pv}E\rvert/(hc\,cm^{-1})$	Reference
CHF═C═CHF	1.4×10^{-13}	141, 143, 151
CHF═C═CHCl	7×10^{-13}	143, 151
CHCl═C═CHCl	1.1×10^{-12}	143, 151
$PF^{35}Cl^{37}Cl$	2.8×10^{-14}	160
CHFClBr	1.9×10^{-12}	40, 99, 127
CDFClBr	1.9×10^{-12}	127, 163
F-oxirane	1.7×10^{-13}	100, 146, 148
D-oxirane	$(2\times10^{-16})^{c}$	167,183
Cyano-oxirane	1×10^{-13}	93, 168
Cyano-aziridine	1×10^{-13}	93
CHDTOH[a]	3.66×10^{-17}	134
Alanine[b]	$\approx5\times10^{-14}$	34, 33, 92

[a]Value for one of two prominent conformers (see ref. 134).
[b]Very strongly conformer dependent with even sign changes when rotating the –COOH group without changing enantiomeric structure (see ref. 92)
[c]Preliminary estimate, the vibrationally averaged value is larger.

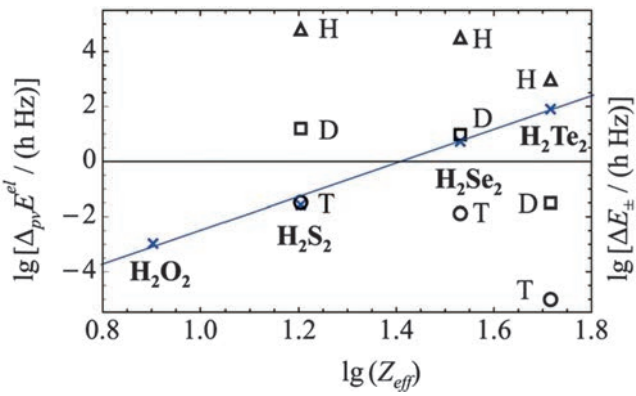

Figure 6.8 Doubly logarithmic representation of the parity-violating energy differences $\Delta_{pv}E^{el}$ (as decadic logarithm, lg, electronic contribution from the parity-violating potential differences) as a function of lg Z_{eff} in the series $^{1,2,3}H–X–X–^{1,2,3}H$ with X = O, S, Se, Te and taking $Z_{eff} = Z_X$ as the effective nuclear charge number (crosses '×' for all isotopomers after ref. 158). $\Delta_{pv}E^{el}$ is essentially independent of the hydrogen isotope. This is compared with tunnelling splittings ($\Delta E_{\pm}$) where the dependence on the hydrogen isotope is essential (triangles for H, squares for D, circles for T). The results are from the summary in ref. 27, where the calculations for $\Delta_{pv}E^{el}$ were taken from Berger and Quack (2000)[35] for H_2O_2 and H_2S_2, (also from Bakasov *et al.* (2004)[128]). The results for $\Delta_{pv}E$ H_2Se_2 and T_2Se_2 are from Laerdahl and Schwerdtfeger (1999)[88] and the tunnelling splittings ($\Delta E_{\pm}$ were taken from Quack and Willeke (2003),[138] Gottselig *et al.* (2001),[89] (2003),[173] and (2004).[135] The slope of the straight-line fit is about 4.8, corresponding to about the Z_{eff}^5 law (see, however, the discussion in ref. 128).

Table 6.2 corresponds to a value near to the maximum of $\Delta_{pv}E$ as a function of the stereomutation reaction coordinate.

The moderately large value of $\Delta_{pv}E$ for the isotopically chiral molecule $PF^{35}Cl^{37}Cl$ is an example of the fundamentally new isotope effect introduced by the electroweak interaction in isotopically chiral molecules as discussed in more detail in ref. 29, 41 and 160. It arises from the difference of the weak nuclear charges of isotopes in eqn (6.13).[160]

6.4 The Quantum Wavepacket Dynamics in Chiral Molecules Where Either Tunnelling or Parity Violation Dominates

6.4.1 Exact and Approximate Studies of Tunnelling in Prototypical Molecules with Transient Chirality: Hydrogen Peroxide and Ammonia Isotopomers

Figure 6.9 shows the H_2O_2 molecule with the two enantiomers in their equilibrium geometry. This was to our knowledge the first example where a reaction of stereomutation was described on a full-dimensional potential surface with all six internal degrees of freedom[131] and a quantum mechanical treatment with exact DVR methods for the spectroscopic stationary states and the time-dependent wave packet dynamics of the tunnelling process.[132,169] Hydrogen peroxide is well suited as a prototype molecule for such investigations due to the large tunnelling splitting of *ca.* 10 cm^{-1} in the ground state that leads to the result that effectively a quantum dynamics in the spirit of Hund is valid independent of the also existing, but for the dynamics, negligible, parity violation (see below).[33–35] In Table 6.4 the

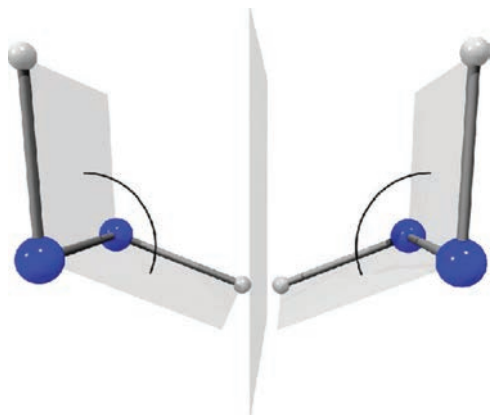

Figure 6.9 H_2O_2 in its two enantiomeric equilibrium geometries, P-enantiomer on the left, M-enantiomer on the right connected by a fast-tunnelling reaction. Reproduced from ref. 161 with permission from Leopoldina, Copyright 1999. See also ref. 131, 132 and 169.

Table 6.4 Tunnelling splittings for H_2O_2 from the numerically exact solution ($\Delta\tilde{\nu}_i^{6D}$), from the quasiadiabatic channel RPH approximation ($\Delta\tilde{\nu}_i^{RPH}$), and from experiment ($\Delta\tilde{\nu}_i^{exp}$). T^{6D} is the tunnelling transfer time. Adapted from ref. 132 and 169 with permission from Elsevier, Copyright 1999, 2007. ω_i is the harmonic wave number of the mode i and $\tilde{\nu}_i^{exp}$ is its experimental fundamental wave number $\tilde{\nu}_i^{6D}$ exact six-dimensional result from theory on the surface from ref. 131.

i	ω_i/cm^{-1}	$\tilde{\nu}_i^{exp}/cm^{-1}$	$\tilde{\nu}_i^{6D}/cm^{-1}$	$\Delta\tilde{\nu}_i^{exp}/cm^{-1}$	$\Delta\tilde{\nu}_i^{6D}/cm^{-1}$	$\Delta\tilde{\nu}_i^{RPH}/cm^{-1}$	T^{6D}/ps
0	0	0	0	11.4	11.0	11.1	1.5
1	3778	3609.8	3617.7	8.2	7.6	8.4	2.2
2	1453	1395.9	1392.0	(2.4?)	6.1	5.0	2.7
3	889	865.9	850.5	12.0	11.1	10.8	1.5
4	392	254.6	259.3	116	118	120	0.14
5	3762	3610.7	3605.8	8.2	7.4	7.4	2.0
6	1297	1264.6	1236.5	20.5	20.8	21.8	0.8

tunnelling splittings from the numerically exact solution are compared to the approximate results from the quasiadiabatic channel reaction path Hamiltonian (RPH) approach and to experimental results. The strongly mode selective tunnelling times as a function of the excitation of the different degrees of freedom can be recognized. Thus by exciting various vibrational modes, say with a pulsed laser, one can control the stereomutation rates. For example the excitation of the OH-stretching vibrations ν_1 and ν_5 results in a slowing down of the tunnelling process even though the excitation energy is a multiple of the barrier height; it remains an effectively quasiadiabatic process with a slightly modified effective quasiadiabatic channel potential and moment of inertia (''quasi'' tunnelling mass), which is slightly increased by the excitation of an OH-stretching vibration. These two effects together explain qualitatively the slowing down of the process. Similar effects have been found for the inversion motion in the aniline isotopomers (with the chiral isotopomer C_6H_5NHD)[170,171] which shows such a mode-selective ''non-statistical'' tunnelling process with a slowing down after NH-stretching excitation, despite the very high density of states at high excitation in C_6H_5NHD, with good agreement between experimental results and quasiadiabatic channel RPH calculations carried out *ab initio*. While the quasiadiabatic channel RPH treatments have been found to be quite successful in handling multidimensional tunnelling problems, one should bear in mind their approximate nature. The use of ''quasiadiabatic'' in the model is motivated by the approaches of ref. 132, 169, 196 and 207 using an important ''diabatization'' step as compared to the RPH treatment of Miller *et al.*,[208] which might be called rigorously adiabatic. The ''diabatization'' uses the concept of the statistical adiabatic channel model to allow channel potentials of the same symmetry to cross in order to retain their physical nature in terms of the channel wave function.[209] As one might call these crossing ''diabatized'' channels also ''adiabatic'' (with different definitions) we introduced the term quasiadiabatic for them (see ref. 210 for a discussion).

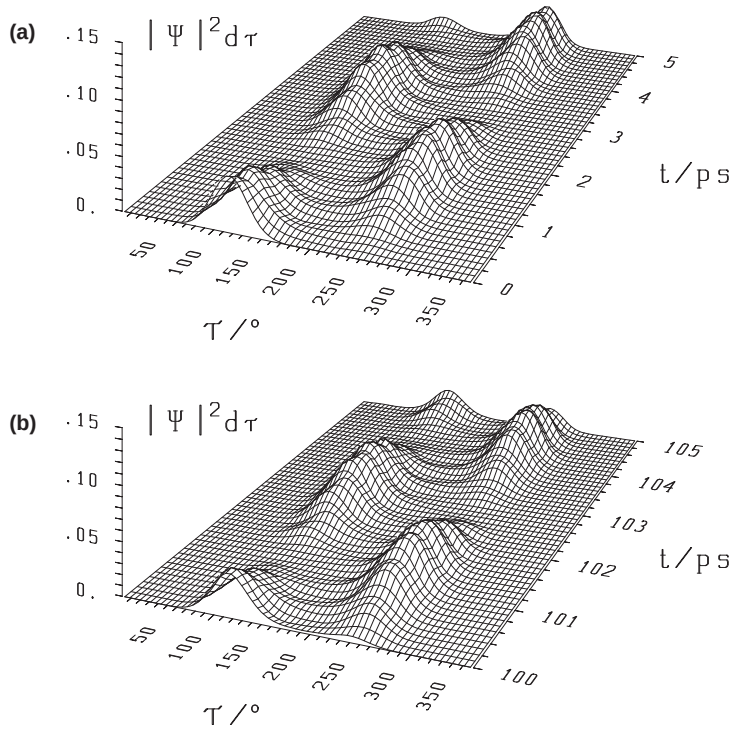

Figure 6.10 Six-dimensional wave packet evolution for H_2O_2 in its lowest quantum states ($i = 0$ in Table 6.4). $|\Psi|^2$ shows the time-dependent probability as a function of the torsional coordinate, where the probability density is integrated over all other coordinates. (a) shows the time interval 0–5 ps and (b) the time interval 100–105 ps with identical initial conditions at $t = 0$ as in (a).[132,169] The migration of the wave packet from the left to the right corresponds to a change from one enantiomer to the other in Figure 6.9.

Figure 6.10 shows as an example the ''wave packet dynamics'' in the ground state of the H_2O_2 molecule in terms of the six-dimensional quantum mechanical probability density as a function of the torsional angle (integrated over the other five degrees of freedom). One can see the initially, at time $t = 0$, ''left''-localized density which shows an approximately Gaussian shape around the equilibrium geometry of the ''left'' enantiomer and which after 1.5 ps transforms to the ''right''-localized wave packet close to the equilibrium geometry of the second (''right'') enantiomer.

The detailed full-dimensional analysis of the wave packet dynamics can be used to test the validity of the quasiadiabatic channel-RPH approximation, which turns out to be a remarkably good approximation for this example. Even at high energies one finds indeed quasi-adiabatic tunnelling above the barrier. The different tunnelling velocities for various excitations of different channels in all possible degrees of freedom can be used for a ''mode

selective'' tunnelling control of the reaction velocity, for instance with the help of laser excitation.[152,172]

As seen from Table 6.4 the excitation of the ''fundamental ν_6'' leads to an enhancement of the tunnelling rate by a factor of 2 while excitation of the torsional mode ν_4 results in an increase in the tunnelling rate by a factor of 10 and the quasiadiabatic channel RPH result is within 5% of the exact result. The time-dependent wave packets from the exact and approximate results are virtually indistinguishable by eye, although the small numerical differences can, of course, be established.[169] The same would be true if one included the parity-violating potentials in the calculation. While rotation was treated approximately in refs. 132,169 in the recent work on tunnelling in ammonia isotopomers all degrees of freedom (vibration and rotation) were treated numerically exactly in a nine-dimensional vibration-rotation-tunnelling calculation.[172] In addition to tunnelling wave packets in the isolated ammonia isotopomers the control of tunnelling rates by well-designed electromagnetic (laser) radiation fields was studied in this work. Figure 6.11 shows the tunnelling enhancement achieved for the chiral isotopomer NHDT, where, with a suitable laser excitation, a transfer time of 40 ps can be obtained compared to a transfer time of 150 ps in the isolated NHDT molecule in its ground state. In addition to this change of the time scale by almost a factor of 4, the minor differences in the shape of the wave packets in the two parts of Figure 6.11 indicate the participation of excited states when including laser excitation.

For a detailed discussion of the fully nine-dimensional tunnelling quantum dynamics of prototype molecule NH_3 and its various deuterium (D), tritium (T), and muonium (Mu) isotopomers under coherent radiative excitation we refer to ref. 172. While ground state tunnelling in ammonia isotopomers is well described by the quasiadiabatic channel reaction path Hamiltonian, there are several excited states where this approximation is insufficient due to strong effects from intramolecular vibrational redistribution,[172,177] which are not included in the ordinary quasiadiabatic channel RPH treatment, although they might, in principle, be included in an extended approach that takes into account such couplings on a case-specific basis.

As can already be seen from the overview in Table 6.2, molecules such as HOOH and NHDT, which are chiral in the equilibrium geometry, but have tunnelling splittings in the ground state on the order of cm^{-1} and have only an exceedingly small effect from parity violation, the tunnelling sublevels have essentially a well-defined parity and the eigenstates are essentially ''achiral'', although they have a small admixture of the ''wrong'' parity and are very slightly optical active. The truly chiral superposition states are short lived (ps to μs, say) and thus one may call these molecules ''transiently chiral'' due to tunnelling, although they would be stable chiral molecules at their minima within classical molecular dynamics. Transiently chiral molecules can show a large optical activity like ordinary chiral molecules, but with a time dependence following the wave packet dynamics. The tunnelling dynamics of transiently chiral molecules is qualitatively similar to the

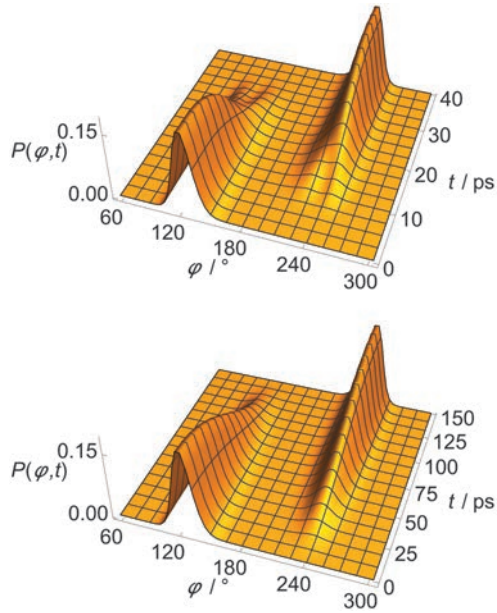

Figure 6.11 Reduced probability density as a function of the inversion coordinate φ and time t for NHDT. The two enantiomeric structures correspond to $\varphi \cong 120^\circ$ and $\varphi \cong 240^\circ$, respectively. The upper and lower panels show reduced probability densities (probability densities integrated over all other coordinates) for the tunnelling enhancement (upper) and field-free (lower) dynamical schemes, respectively. The parameters of the laser pulse are $\tilde{\nu}_0 = 793.5\ \mathrm{cm}^{-1}$, $I_{\max} = 3.15\ \mathrm{GW\,cm}^{-2}$, and $t_p = 40$ ps. Reproduced from ref. 172 with permission from AIP Publishing, Copyright 2019.

tunnelling dynamics of achiral molecules such as NH_3, NHD_2,[172] or phenol[179] as far as parity violation is concerned, which for many applications can be neglected in the quantum dynamics of these molecules, although parity violation leads to some very weak effects also in these cases.

6.4.2 Tunnelling in Chiral Molecules Where Parity Violation Dominates Over Tunnelling

Ordinary stable chiral molecules have lifetimes on the order of at least some days (say $\tau > 10^6$ s) and thus tunnelling splittings of less than $10^{-17}\ \mathrm{cm}^{-1}$, which implies that with typical values of parity-violating energy differences of $|\Delta_{pv}E| > 10^{-14}\ \mathrm{hc\,cm}^{-1}$ parity violation dominates over tunnelling, eqn (6.31). Therefore the eigenstates are essentially localized in chiral R or S structures (or P and M for axially chiral molecules). This by itself demonstrates the perhaps surprising fact that parity violation is a dominant factor in the quantum dynamics of ordinary chiral molecules.[36,149] Figure 6.12 shows the situation for the molecule Cl-SS-Cl,

which has negligible tunnelling in the ground state and up to very high torsional excitation (the highest level shown in Figure 6.12 has torsional quantum number $v_T = 80$, still well below the *trans* barrier for stereomutation, which is calculated to be higher than 5000 cm^{-1} in this molecule). This example shows several features that are frequently

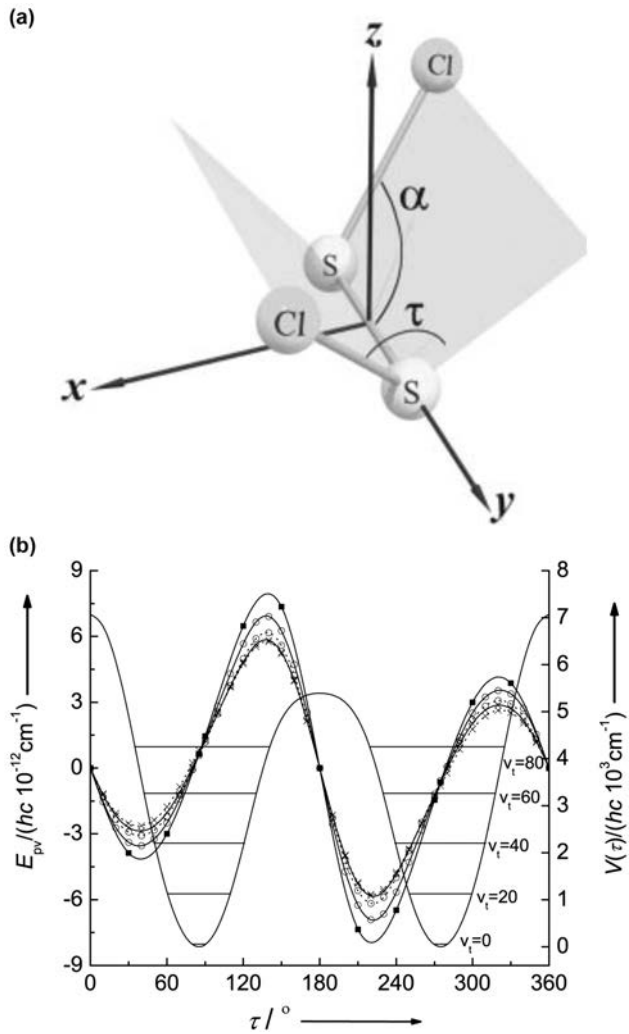

Figure 6.12 (b) Calculated torsional potential (full line, right ordinate scale) and parity-violating potential (left ordinate scale, lines with various symbols for various approximations in the electroweak quantum chemistry[90]) for ClSSCl, where the equilibrium structure and the definition of the torsional angle τ are shown in (a).
Reproduced from ref. 90 with permission from John Wiley and Sons, © 2001 WILEY-VCH Verlag GmbH, Weinheim, Fed. Rep. of Germany, and from ref. 178 with permission from CHIMIA, Copyright 2003 (where one finds a detailed discussion).

encountered. Firstly, there is a strong dependence of the parity-violating potential, which is antisymmetric with respect to inversion at the achiral geometry 180°, upon the torsional angle τ. The parity-violating potential vanishes by symmetry at the achiral planar geometries of the molecule. However, the parity-violating potential also vanishes ''accidentally'' at some chiral geometries ($\tau \approx 80^\circ$ and 240°). This perhaps at first sight surprising phenomenon is rather frequently observed in the theory of parity violation in chiral molecules and has been discussed in ref. 33, 34, 83 and 84 in terms of the tensor properties of the parity-violating potential. The P enantiomer is stabilized (negative E_{pv}) compared to the M enantiomer for values of $0^\circ < \tau < 80^\circ$ and P is destabilized (positive E_{pv}) compared to M for $80^\circ < \tau < 180^\circ$. Thus, at the equilibrium geometry near $\tau \approx 85^\circ$ the M enantiomer is more stable than the P enantiomer by about $10^{-12}\,\mathrm{cm}^{-1}$. Figure 6.12 shows also the effect using different levels of quantum chemical accuracy in the calculation of the parity-violating potentials. For the optimized equilibrium structures on finds values for the parity violating energy difference in the range $1.14 \leq \Delta_{pv}E/(\mathrm{hc\,cm}^{-1} * 10^{-12}) \leq 1.62$ at various levels. At the RPA-cc-pvTZ-A level one has at the equilibrium geometry $\Delta_{pv}E/(\mathrm{hc}) = 1.29 \times 10^{-12}\,\mathrm{cm}^{-1}$. If one calculates the two lowest eigenstates in the effective torsional potential with parity-violating potential included one finds an energy difference $\Delta_{pv}E/(\mathrm{hc}) = 1.35 \times 10^{-12}\,\mathrm{cm}^{-1}$ between the two lowest states with effectively localized eigenfunctions. If one calculates the expectation value over the parity-violating potential in the ground state wave function in one well and then $\Delta_{pv}E^{(0)}$ from eqn (6.29) one finds exactly the same values $1.35 \times 10^{-12}\,\mathrm{cm}^{-1}$ as expected.[90]

Finally, one may wish to compare to the tunnelling splitting $\Delta E_\pm$ in the hypothetical symmetric potential without parity violation. It turns out that numerical limitations prohibit a direct calculation with, say, the quasiadiabatic channel RPH method, because of the extremely small absolute magnitude of $\Delta E_\pm$. Therefore in ref. 90 a scaling and extrapolation method was developed that uses quasiadiabatic channel RPH calculations in a range where they are accurate in scaled torsional potentials

$$V(\tau, f) = fV(\tau) \tag{6.44}$$

with a scaling factor f that reduces the barrier height accordingly. Accurate results for $\Delta E_\pm(f)$ with different scaling factors f are then fitted to a three-parameter expression ($\lg = \log_{10}$)

$$\lg\left|(\Delta E_\pm(f)/(\mathrm{hc\ cm}^{-1}))\right| = P_1 \lg\sqrt{f} + P_2 - P_3\sqrt{f}. \tag{6.45}$$

This gives then a value for $\Delta E_\pm$ extrapolated to $f = 1$

$$\Delta E_\pm(f = 1) = (\mathrm{hc})10^{P_2 - P_3}\ \mathrm{cm}^{-1}. \tag{6.46}$$

This fit formula is motivated by a WKB approximation result for tunnelling splittings in symmetric double-well potentials $V(x)$.[90,184]

$$\Delta E_\pm = (h\omega/\pi)\sqrt{2m\omega a^2/h}\,\exp(-2\pi A S_0/h). \tag{6.47}$$

The terms S_0 and A arise from the WKB theory with the classical angular oscillation frequency ω of the harmonic small amplitude motion around the quadratic well at $x = a$ and $x = -a$, and m is the reduced mass with furthermore:

$$S_0 = \int_{-a}^{a} \sqrt{2mV(x)}\, \mathrm{d}x \tag{6.48}$$

$$A = \int_{0}^{a} [m\omega/(2mV(x)) - 1/(a - x)]\mathrm{d}x. \tag{6.49}$$

Scaling of the symmetric double-well potential $V(f, x) = f\,V(x)$ results in a classical scaled $\omega(f) = \sqrt{f}\omega(f = 1)$. Insertion of $V(f, x)$ and $\omega(f)$ into the WKB approximation for $\Delta E_{\pm}$ gives the ground state tunnelling splitting as a function of the scaling factor f, which can be written in the form of the fit formula with $P_1 = 3/2$ and $P_2 = \lg\left((h\omega/\pi)\sqrt{2m\omega a^2/h}\exp(A)/\mathrm{J}\right)$ and $P_3 = 2\pi S_0/(h \ln 10)$. However, rather than using the ''theoretical'' values for P_1, P_2, and P_3, which would limit the result to the simple WKB model neglecting details of the potential, the fit includes the properties of the tunnelling dynamics in the real potential by allowing the freely floating parameters to account for the dynamics at least to a reasonable extent. In this way a value of $\Delta E_{\pm} = (\mathrm{hc})10^{-76}\,\mathrm{cm}^{-1}$ is obtained. Figure 6.13 shows the fit of the equation with the parameters $P_1 = 1.16(5)$, $P_2 = 2.59(10)$, and $P_3 = 78.73(24)$ to numerically calculated (''accurate'') points.

Obviously one does not have to know the exact values of the extremely small tunnelling splittings to ascertain the validity of the inequality (6.31).

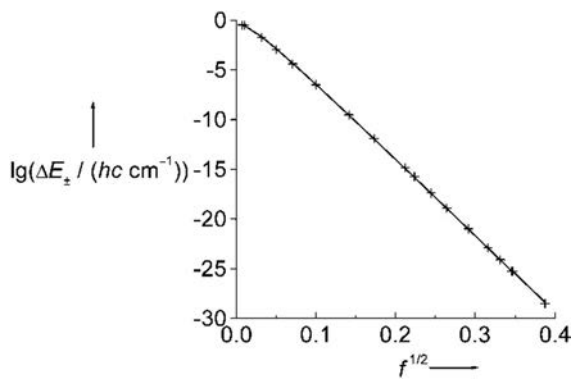

Figure 6.13 Decadic logarithm of the torsional tunnelling splittings $\Delta E_i(f)$ for differently scaled torsional potentials $V(\tau, f) = fV(\tau)$ calculated with the quasiadiabatic channel-reaction path Hamiltonian approach (+ for RPH) and fit to eqn (6.45) (line).
Reproduced from ref. 90 with permission from John Wiley and Sons, © 2001 WILEY-VCH Verlag GmbH, Weinheim, Fed. Rep. of Germany.

However, the method presented in ref. 90 can be generally useful in the computation of very small tunnelling splittings. The fitting, interpolation and extrapolation method can be applied to the analysis of many numerically exact multidimensional approaches to tunnelling.

6.4.3 Tunnelling Switching in Chiral and Achiral Molecules

For chiral molecules where in the ground state the tunnelling is effectively suppressed because of the parity-violating asymmetry and the eigenstates are localized essentially near either one or the other potential minimum, one can increase the efficiency of tunnelling by vibrational excitation of modes that promote tunnelling, notably the modes that closely correspond to the reaction coordinate for stereomutation, the torsional mode in HOOH and HSSH and the inversion mode in ammonia NHDT, for example; as already discussed. Thus, at sufficiently high excitation tunnelling will always dominate over parity violation, leading to stereomutation or racemization by tunnelling.[41] This phenomenon has been studied quantitatively for the molecule ClOOCl, which in the vibrational ground state is dominated by parity violation, with therefore localized chiral eigenstates at $v = 0$ (as also seen from Table 6.2).[150–152] The vibration-rotation-tunnelling problem was treated including all vibrational degrees of freedom in the quasiadiabatic channel RPH approximation.[132,136,152] Rotation was treated with a Watson-type Hamiltonian[180] and the WANG program[185] using rotational constants computed from the expectation values in the vibrational states resulting from the quasiadiabatic channel RPH calculations and neglecting the effects of nuclear hyperfine structure. At a torsional level of $v = 10$ the tunnelling splitting is calculated to be about $2 \times 10^{-7}\,\mathrm{cm}^{-1}$, thus dominating by far over the parity violation [$\Delta_{pv}E \cong (hc)\ 5 \times 10^{-13}\,\mathrm{cm}^{-1}$, about 15% smaller than in the vibrational ground state, computed at the MC-LR RPA/6-311+G(3df) level[152]]. Exciting coherently to $v = 10$ with a 5 μs laser pulse ($\tilde{\nu}_L = 1104.2586\ \mathrm{cm}^{-1}$, $I_{max} = 30\ \mathrm{MW\,cm}^{-2}$) giving a power broadening of $3.9 \times 10^{-6}\,\mathrm{cm}^{-1}$, much larger than the tunnelling splitting, one generates a highly excited, localized chiral torsional state, which shows field-free tunnelling stereomutation after the laser pulse is switched off. The scheme of excitation is shown in Figure 6.14 and the stereomutation wave packet is shown as probability density in the torsional coordinate (integrated over all other coordinates) in Figure 6.15. This excited state wave packet is comparable to the ground state wave packet shown for HOOH in Figure 6.10. The structure of the probability density is more complicated because of the high torsional excitation, but the effects of parity violation, while included, are not visible on the scale of Figure 6.15. One has essentially a periodic stereomutation motion with a period of about 200 μs, in agreement with eqn (6.1), easily seen in the time range 20–220 μs in the later part of Figure 6.15.

However, when selectively exciting with a narrow bandwidth laser pulse ($\tilde{\nu}_L = 1186.7912\ \mathrm{cm}^{-1}$, $I_{max} = 0.5\ \mathrm{GW\,cm}^{-2}$, 5 μs) to a tunnelling sublevel at

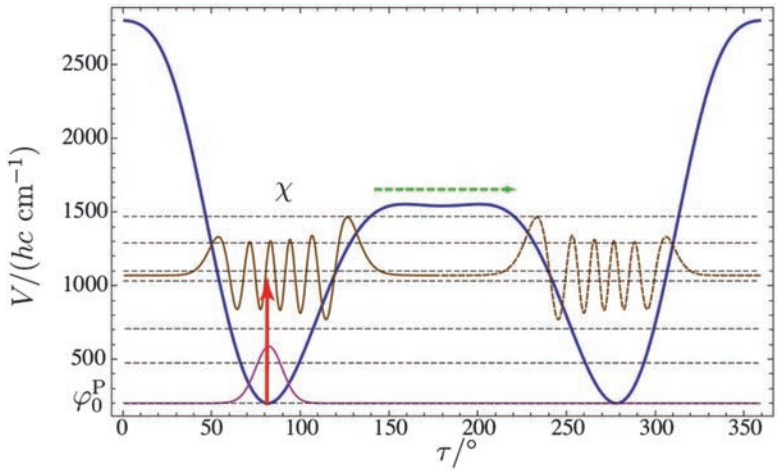

Figure 6.14 Excitation scheme: starting with a chiral ground state, a chiral state $\chi(v=10)$ near the barrier is populated after laser irradiation. After the excitation of χ, one expects tunnelling stereomutation (TSM) during field-free evolution, because χ is a superposition of two parity eigenstates.
Reproduced from ref. 152 with permission from American Chemical Society, Copyright 2015.

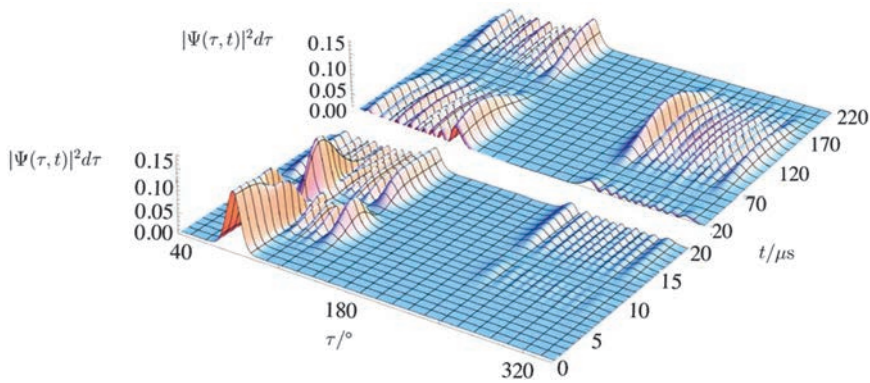

Figure 6.15 Time-dependent wave packet for $0 \le t \le 220$ μs with $d\tau = \Delta\tau = 1^\circ$. Early times: wave packet during excitation. After about 15 μs, the laser field is off and field-free evolution starts, which will eventually lead to tunnelling stereomutation (TSM) of the chiral state χ. Later times: wave packet showing TSM during field-free evolution of the molecular state. The period is roughly 200 μs, in accordance with eqn (6.1).
Reproduced from ref. 152 with permission from American Chemical Society, Copyright 2015.

$v_T = 11$ ($\Delta\tilde{\nu}_T = 1.2\times10^{-4}\,\mathrm{cm}^{-1}$) followed by a transfer pulse (593.8252 cm^{-1}, 1.6 MW cm^{-2}, 5 μs) one generates initially a state with well-defined parity after the transfer in $v_T = 5(\Delta\tilde{\nu}_T = 9.5\times10^{-17}\,\mathrm{cm}^{-1})$ where parity violation dominates ($\Delta_{pv}E = 5.5\times10^{-13}(\mathrm{hc})\,\mathrm{cm}^{-1}$). This state will thus slowly change

parity following eqn (6.43) giving a population of about 2.5×10^{-7} after some milliseconds for the initially ''forbidden'' parity, a detectable signal according to the scheme of ref. 41 and 149 and current techniques.[181] The quantum dynamical simulations presented in ref. 152 are the first of their kind treating coherent excitation, vibration-rotation-tunnelling dynamics and electroweak parity violation together and demonstrating experimentally detectable effects. They constitute a realistic simulation of one of the experimental approaches to be discussed in Section 6.5 in more detail.

Tunnelling switching has been identified quantitatively by theory and high-resolution spectroscopy in the achiral molecule *m*-D-phenol, where one has stereoisomers (*syn*-, *anti*-). There it has been proposed for potential use in quantum technology as a molecular quantum switch.[186,187]

Tunnelling switching has also been discussed for partially deuterated or halogenated ethylene isotopomers[157] and recently for the mono deuterated vinyl radical CHD=CH by *ab initio* calculations,[188] see also the review[223] in the current book. A simple stable closed-shell example would be an imine CHD=NH, which also has *syn*- and *anti*-isomers depending upon the relative position of NH with respect to D. The particular property of a quantum switch as compared to a ''classical'' molecular switch[189] is the possibility of generating the bistructural superposition states of *syn*- and *anti*-isomers, analogous to the bistructural superposition of *R*- and *S*-enantiomers.[41,149,158] For a more detailed discussion of tunnelling motion in asymmetric potentials we refer to general reviews.[14,15] The new concept of bistructural (and possibly multistructural) states in stereochemistry has also been discussed[190] in a broader context of the historical developments of concepts in chemistry. The molecular quantum switch offers many new possibilities for quantum technology, going beyond the quasiclassical molecular switches, which have been so much investigated.

It has also a so far hypothetical importance for a molecular theory of vision and thought including the question of ''free will''.[42,110]

6.4.4 Tunnelling Stereomutation and Racemization Kinetics in Chiral Molecules

The general problem of tunnelling stereomutation and racemization has been discussed in ref. 41 for the case that either $\Delta E_{\pm}$ or $\Delta_{pv}E$ or both are very small compared to other energy level spacings, and we briefly summarize the treatment given therein as it provides useful insight. In this case one can treat the kinetics by considering an ensemble of near-degenerate two-level systems. The Hamiltonian matrix has the form (6.50). The eigenvalues for a Hermitian operator (6.51) follow from (6.52).

$$\hat{H} = \begin{pmatrix} H_{11} & H_{12} \\ H_{21} & H_{22} \end{pmatrix} \tag{6.50}$$

$$H_{12}H_{21} = H_{12}H_{12}^{*} = |H_{12}|^2 \tag{6.51}$$

$$E_{1,2} = (H_{11} + H_{22})/2 \pm \frac{1}{2}[(H_{11} - H_{22})^2 + 4|H_{12}|^2]^{1/2} \tag{6.52}$$

If we work in the basis $\chi_\pm$ of states of well-defined parity and introduce $\Delta_{pv}E$ as a perturbation parameter, one may identify the matrix elements (with real H_{12} and positive $\Delta E_\pm$) in eqn (6.53) and (6.54)

$$\Delta_{pv}E = 2H_{12} \tag{6.53}$$

$$H_{11} = E_\pm/2 = -H_{22}. \tag{6.54}$$

If $\Delta E_\pm$ is much larger then $\Delta_{pv}E$, the latter is not a measurable energy difference. If we work in the basis of ''left'' and ''right'' handed states λ and ρ one has (positive $\Delta_{pv}E$), and the eqn (6.55) and (6.56), introducing now $\Delta E_\pm$ as the perturbation (much smaller now than $\Delta_{pv}E$)

$$H'_{11} = \Delta_{pv}E/2 = -H'_{22} \tag{6.55}$$

$$\Delta E_\pm = 2H'_{12}. \tag{6.56}$$

The eigenvalues given by eqn (6.57) with respect to the average energy $(E_1 + E_2)/2 = \langle E \rangle \equiv 0$ are obviously the same [$\Delta E_\pm$ and $\Delta_{pv}E$ are defined as real, positive, eqn (6.57)]. It is immaterial, whether $\Delta_{pv}E$ or the tunnelling $\Delta E_\pm$ is introduced as ''perturbation''

$$E_{1,2} = \langle E \rangle \pm \frac{1}{2}(\Delta E_\pm^2 + \Delta_{pv}E^2)^{1/2}. \tag{6.57}$$

Eigenvectors for the example of basis χ are given by eqn (6.58) where x and y are defined *via* S [eqn (6.59)] according to eqn (6.60) and (6.61)

$$\boldsymbol{C} = \begin{pmatrix} x & y \\ -y & x \end{pmatrix} \tag{6.58}$$

$$S = (\Delta E_\pm^2 + \Delta_{pv}E^2)^{1/2} \tag{6.59}$$

$$x^2 = (S + \Delta E_\pm)/(2S) \tag{6.60}$$

$$y^2 = (S - \Delta E_\pm)/(2S) \tag{6.61}$$

The sign of the roots $\sqrt{x^2}$ and $\sqrt{y^2}$ can be taken in various combinations respecting $\boldsymbol{C}^T\boldsymbol{C} = \mathbf{1}$ (S is defined positive). One has by convention $E_1 < E_2$ and $H_{11} < H_{22}$. Figure 6.7 represents the situation [$x = y = 1/\sqrt{2}$, right-hand side of Figure 6.7, and the wave functions are given by eqn (6.33)–(6.36)].

According to the superposition principle (if valid) these states can always be generated. The time evolution is given by the time evolution matrix in eqn (6.62).

$$\boldsymbol{U} = \boldsymbol{C}\begin{pmatrix} \exp(-\mathrm{i}2\pi E_1 t/h) & 0 \\ 0 & \exp(-\mathrm{i}2\pi E_2 t/h) \end{pmatrix}\boldsymbol{C}^{\boldsymbol{T}}. \tag{6.62}$$

The density matrix with the elements $P_{ij} = \langle c_i c_j^* \rangle$ ($\langle\rangle =$ average over an appropriate ensemble) has the form given by eqn (6.63) in the basis λ, ρ and the form of eqn (6.64) in the $\chi_\pm$ basis

$$\begin{pmatrix} P_{\mathrm{RR}} & P_{\mathrm{RL}} \\ P_{\mathrm{LR}} & P_{\mathrm{LL}} \end{pmatrix} = \boldsymbol{P}^{\boldsymbol{\lambda,\rho}} \tag{6.63}$$

$$\begin{pmatrix} P_{++} & P_{+-} \\ P_{-+} & P_{--} \end{pmatrix} = \boldsymbol{P}^{\boldsymbol{\chi}_\pm}. \tag{6.64}$$

For the degenerate system (or nearly degenerate system) at any temperature $kT \gg \Delta E$ or S, eqn (6.65) holds

$$\boldsymbol{P}^{\boldsymbol{\lambda\rho}} = \boldsymbol{P}^{\boldsymbol{\chi}_\pm} = \begin{pmatrix} 1/2 & 0 \\ 0 & 1/2 \end{pmatrix}. \tag{6.65}$$

$\boldsymbol{P}$ is invariant under the basis transformation (as any other constant diagonal matrix), also in the many-level case, if $\boldsymbol{H}$ is block diagonal with some constant in each block. A racemic mixture of R and L is identical to a mixture of + and – in terms of any observable ensemble property. A common model for $\boldsymbol{P}$, simplified for the degenerate case, considered as reduced density matrix of the molecule interacting by collisions or otherwise with a thermal bath gives the eqn (6.66) and (6.67), from which the eqn (6.69) and (6.70) can be derived for the relaxation times given by τ_1 and τ_2 with the basis transformation in eqn (6.68).

$$(P_{11} - P_{22}) = (P_{11}^0 - P_{22}^0)\,\exp(-t/\tau_1) \tag{6.66}$$

$$P_{12} = (P_{12}^0\,\exp(-t/\tau_2) \tag{6.67}$$

$$P^{\chi_\pm} = \boldsymbol{C}\boldsymbol{P}^{\boldsymbol{\lambda,\rho}}\boldsymbol{C}^{\boldsymbol{T}} \tag{6.68}$$

$$\tau_1^{\chi_\pm} = \tau_2^{\lambda,\rho} \tag{6.69}$$

$$\tau_2^{\chi_\pm} = \tau_1^{\lambda,\rho}. \tag{6.70}$$

Here we have made use of the reality of P in the case of a degenerate model, because $E_{1,2}$ can be set to zero without loss of generality. To within this approximation, the assignment of ''phase'' or ''population'' relaxation times τ_1 and τ_2 is arbitrary in the two-level problem. One can get a ''case C'' (ref. 41) type relaxation behaviour in this limit with apparent irreversible racemization.

When the density of rovibronic and hyperfine states becomes very large, the two-level approximation breaks down and one can obtain ''true'' irreversible

relaxation according to a Pauli master equation (case B of ref. 211) as discussed in more detail in ref. 41. When averaging over a large number of levels as appropriate for intramolecular stereomutation kinetics of polyatomic molecules at higher excitation, with either thermal or some other statistical non-thermal populations, one obtains relaxation-like behavior following eqn (6.3) with rate constants k_{RS} and k_{SR}, written explicitly for the elementary steps

$$R \rightarrow S \text{ rate constant } k_{SR} \tag{6.70}$$

$$S \rightarrow R \text{ rate constant } k_{RS}. \tag{6.71}$$

Different from tunnelling stereomutation of isolated levels, which is oscillatory in time, eqn (6.70) and (6.71) describe a relaxation towards a stationary state, possibly microcanonical or thermal equilibrium, depending on the situation. In the general case, however, this relaxation is not simply a first-order kinetics with detailed balance as in an ordinary chemical system. This simple behavior is reached in the limit of ''case B'' and a thermal initial population. We refer to ref. 41, 42, 211 and 217 for further discussion and to ref. 169 for a simulation showing how statistical averaging arises for the special case of HOOH. We note here that, in principle, either oscillatory- or relaxation-like behavior in isolated molecules showing stereomutation could be observed by measuring the time-dependent structure, say by the techniques of ref. 212–214. The alternative would be to measure time-dependent optical activity, Raman optical activity or vibrational circular dichroism,[215] although such experiments have not yet been carried out on isolated molecules. In a historical context, it is of interest that the very first observation and quantitative kinetic analysis was by a measurement of time-dependent optical activity, albeit not in an isolated molecule nor for an elementary reaction but rather for a catalysed reaction in solution[216] (see ref. 178 for a discussion of the history). Indeed, Wilhelmy seems to have been the first to formulate a first-order rate equation and integrate it to get the exponential behavior as described by eqn (6.72) and (6.73) for the time-dependent concentrations c_R and c_S of the R and S enantiomers:

$$-\frac{dc_R}{dt} = +\frac{dc_S}{dt} = k_{SR}c_R - k_{RS}c_S \tag{6.72}$$

$$c_R(t) - c_S(t) = [c_R(t_0) - c_S(t_0)]\ \exp[-(k_{RS} + k_{SR})(t - t_0)]. \tag{6.73}$$

For a discussion of the emergence of this behaviour starting from the Schrödinger equation see ref. 41, 42, 211 and 217.

6.5 Spectroscopic Approaches Towards Tunnelling and Parity Violation in Chiral Molecules

A variety of experimental approaches to detect parity violation in chiral molecules has been proposed. One can find a summary of these in ref. 27, 29, 30, 32, 36, 41, 158, 171 and 176. However, it seems that so far only two of

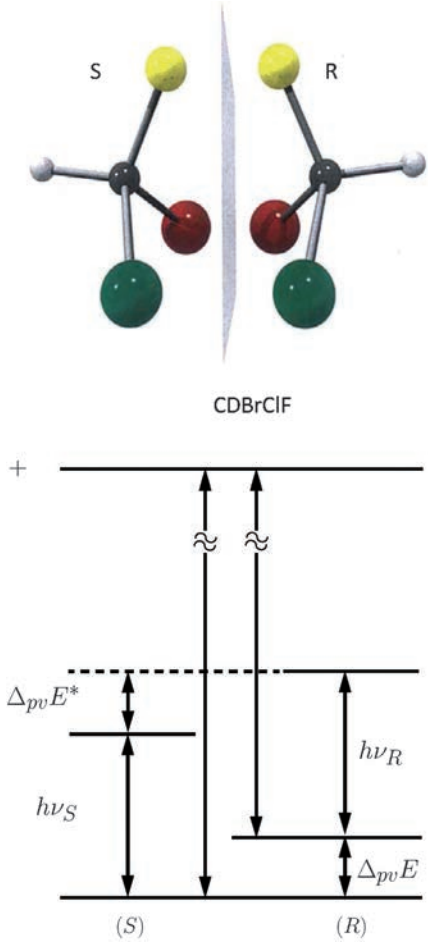

Figure 6.16 Scheme for energy levels and experiments. One notes that $\Delta\nu_{pv} = \nu_R - \nu_S = (\Delta_{pv}E^* - \Delta_{pv}E)/h$ in this scheme.
Reproduced from ref. 29 with permission from the Royal Society of Chemistry, and from ref. 36 with permission from John Wiley and Sons, © 2002 WILEY-VCH Verlag GmbH & Co. KGaA, Weinheim.

these approaches are actively pursued in actual experiments, which may be successful in the foreseeable future, and we restrict our discussion to these, referring to the more complete reviews as mentioned for the larger number of further approaches.

The basic concepts of the current experimental approaches can be understood with the energy level scheme presented in Figure 6.16.

In the first scheme, originally proposed by Letokhov,[51,52] one attempts to measure the frequency difference between spectroscopic transitions, say, in the infrared rotation-vibration spectrum of the separate R and S

enantiomers. CHFClBr was an early IR-laser spectroscopic example[51,52] pursued further in the IR and microwave ranges in ref. 98 and 99 where, by analysis of the spectrum of CHFClBr in the CO_2 laser range, a number of coincidences with laser lines were suggested for ultrahigh-resolution spectroscopy. This provided the starting point for the subsequent study in ref. 101, 102 and 174. Of course other spectral ranges might be studied as well, for instance NMR.[72,73] This ''Letokhov-scheme'' for spectroscopic experiments has two main disadvantages, see ref. 36 and 41 and the critical summary[176] and references cited in ref. 175. Firstly, one cannot derive the parity-violating energy difference $\Delta_{pv}E$, but only the difference of such differences in different states $(\Delta_{pv}E^{*} - \Delta_{pv}E)$. Secondly one has to obtain enantio-pure samples for the two enantiomers.

In ref. 41 and 149 a scheme was proposed that avoids both of these disadvantages and can derive $\Delta_{pv}E$ and $\Delta_{pv}E^{*}$ separately. It makes use of transitions to an intermediate excited state of well-defined parity (labelled + in Figure 6.16) that can result either from tunnelling switching or from an excited electronic state that is planar or quasiplanar as for 1,3-difluoroallene. The scheme is outlined in Figure 6.17.

This allows then for a spectroscopic selection of states of well-defined parity. In a second step, in the scheme of Figure 6.17 one prepares a state of well-defined parity in the ground state (or some other low energy state n), which satisfies the condition

$$\Delta_{pv}E^{(n)} \gg \Delta E_{\pm}^{(n)}. \tag{6.74}$$

The parity selection arises from the electric-dipole selection rule connecting levels of different parity. Thus, if in the first step one has selected a state of some given parity, in the second step one prepares a state of the opposite parity. Such a state is a superposition of the energy eigenstates of the two enantiomers separated by $\Delta_{pv}E$ and therefore shows a periodic time evolution with a period given by eqn (6.32). In such a state parity evolves in time due to parity violation and parity is not a constant of the motion. The probability of finding a given parity (p^{+} for positive parity and p^{-} for negative parity) is given by eqn (6.43).

In the third step, the initially ''forbidden'' population of negative parity $p^{-}(t)$ is probed very sensitively, for example by resonantly enhanced multiphoton ionization (REMPI). This is possible because the line spectra of positive and negative parity isomers are different, with lines that are well separated at high resolution (Figure 6.17 and ref. 181). In this fashion it is not necessary to wait for a whole period, but it is sufficient to probe the initial time evolution at very early times. The sensitivity in the probe step determines, in essence, how small a value of $\Delta_{pv}E$ can be measured. In a recent proof of principle experiment with a current experimental set up in our laboratory on the achiral molecule ammonia, NH_3, it was estimated that an energy difference as small as 100 aeV should be measurable with the existing current experiment.[181] The original proposal[149] of 1986 assumed population transfer using pulse shaping or chirp by rapid adiabatic passage.

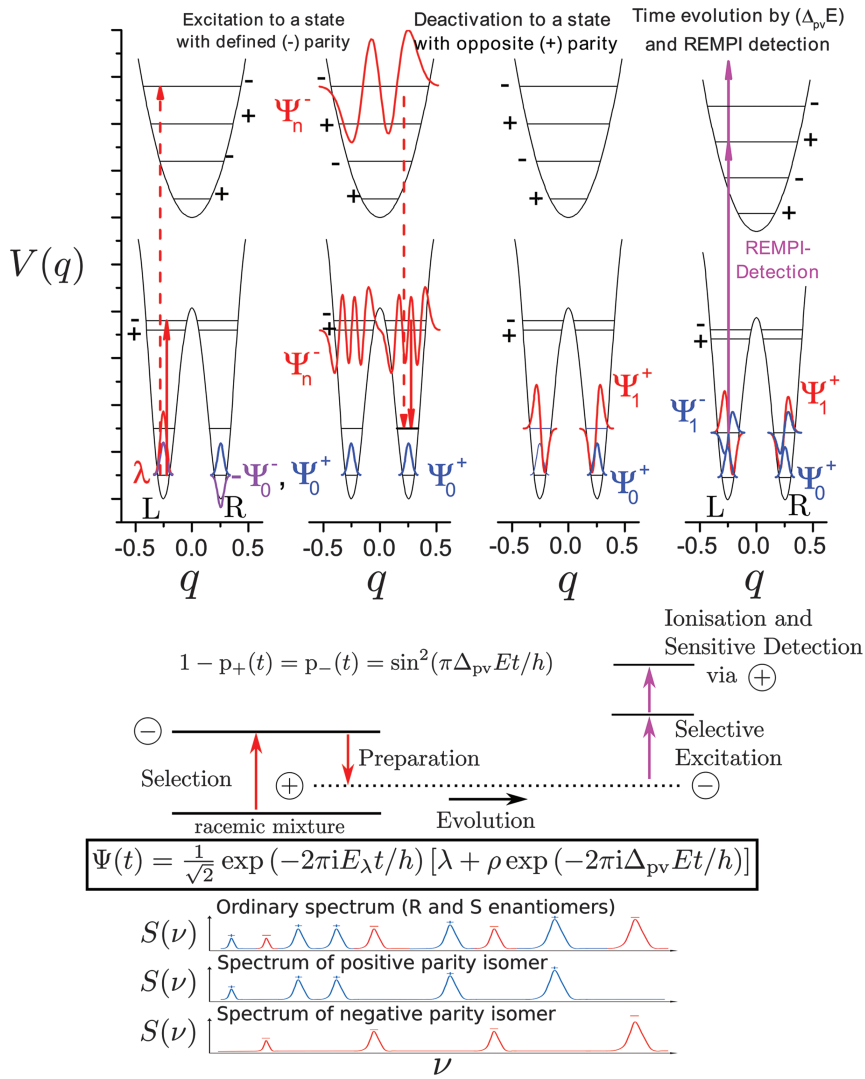

Figure 6.17 Scheme of the preparation and detection steps for the time-resolved experiment to measure $\Delta_{pv}E$. Top: the transitions to the intermediate states are indicated together with the corresponding wave functions for an excited state with well-defined parity close to the barrier of a double minimum potential (full line) or an achiral electronically excited state (dashed line) as an intermediate. The right-hand part shows the sensitive detection step with REMPI. Middle: summary scheme for the three steps. Bottom: the spectra of the normal enantiomers (top) and of the selected positive (blue) and negative (red) parity isomers.
Adapted from ref. 32, 181 and 182 with permission from AIP Publishing, Copyright 2014, 2015, 2019, and from ref. 149 with permission from Elsevier, Copyright 1986.

It is clear, however, that also that the elegant method of stimulated Raman adiabatic passage (STIRAP) as developed later in ref. 194 is an ideal technique for generating population transfer in a well-controlled fashion.[182]

The major current and future challenges are related to the much greater complexity of the rovibrational-tunnelling spectra of chiral molecules as compared to the test molecule NH_3 with its very well-known spectra. However, first spectroscopic investigations on three candidate molecules proved promising (1,2-dithiine $C_4H_4S_2$ and trisulfane HSSSH as well as 1,3-difluoroallene, see Table 6.3). The current cw-OPO laser systems (coupled to a frequency comb) cover only spectral ranges above about 2500 cm^{-1} in the infrared. This limits the choice of molecules. Further development in laser technology, for instance of quantum cascade lasers with power and resolution meeting our needs in the future, might make other molecules accessible, for instance the simpler molecule ClOOCl, for which complete theoretical simulations of the experiment have been achieved already, as discussed in Section 6.4.3.

While the experiment to measure $\Delta_{pv}E$ might have appeared impossible when it was first proposed in 1986,[149] the current outlook on a successful experiment is excellent. Indeed, provided that adequate funding for the continuation of the current project is guaranteed and required spectroscopic analyses can be completed, most significant results can be expected for any of two possible outcomes:

1. Either one finds experimentally the theoretically predicted values for $\Delta_{pv}E$, then one can analyze the results of the precision experiments in terms of the standard model (SMPP) in a range not yet tested by previous experiments.
2. Or else one finds values for $\Delta_{pv}E$ different from the theoretical predictions. This then will lead to a fundamental revision of current theories for $\Delta_{pv}E$ with the potential also for new physics.

In addition, the experimental results will have implications for our understanding the evolution of biomolecular homochirality.[29,31,32,36]

To conclude a note may be useful here on other experiments in physics, and in particular atomic and molecular physics. Indeed, parity violation as discovered in nuclear and particle physics[22–26] has been considered to be rather well understood in the framework of the standard model of particle physics (SMPP) and high energy physics.[43–47,218,219] There have been also successful experiments in atomic spectroscopy (see ref. 220 and 221 and references cited therein) following the early proposals in ref. 121 and 122. There have been also extensive proposals to study parity violation in diatomic molecules, including quite early ones,[222] although until today no successful experiments demonstrating the effect in diatomic molecules have been reported in spite of extensive efforts with null results. We refer to the detailed recent review[221] with some emphasis on experiments on atoms and diatomic molecules.

In agreement with the aim of the present book,[16] our focus has been here entirely on parity violation and its interplay with tunnelling in chiral molecules. Beyond the interest in providing new concepts for physical-chemical stereochemistry, there is also a fundamental aspect in chiral molecules making them rather special in the context of parity violation in atomic and molecular physics in general. Indeed, the strength of parity-violating effects is expected to become large whenever the separation of eigenstates of different parity in the electromagnetic Hamiltonian (say, $\Delta E_{\pm}$) becomes comparable to the absolute value of the coupling matrix element V_{pv} connecting the states with the parity-violating electroweak force or when $|V_{\mathrm{pv}}|$ is even much larger than $|\Delta E_{\pm}|$

$$|\Delta E_{\pm}| \cong |V_{\mathrm{pv}}|. \tag{6.75}$$

While in atoms, and diatomic and some achiral polyatomic molecules one can find states with different parity lying rather close, it is the case of chiral molecules with very slow tunnelling, where the degeneracy becomes almost perfect with $\Delta E_{\pm} \cong 0$, and thus the effect of parity violation is maximum. Experiments of parity violation in atoms have been successful only for heavy atoms, where the theoretical analysis is subject to great uncertainty,[27,220] and no experiment on light atoms are expected in the near future. In contrast our experiment on chiral molecules as described here has an experimentally proven sensitivity to test parity violation in molecules containing nuclei no heavier than chlorine, thus testing parity violation in a new low-energy range.[149,181,182] This is a great advantage compared to the experiments on frequency shifts,[174,224] which might sometime in the future be successful for molecules with heavy transition metal atoms and the like, where large effects are predicted. However, the theoretical analysis will be then subject to even greater uncertainty than for heavy atoms. Thus while such experiments still have interest for chemistry, they are not likely to go beyond what has been achieved in experiments on atoms in terms of a fundamental analysis. In fact the experiment on measuring $\Delta_{\mathrm{pv}}E$ through time-dependent parity seems to be the only one at present with an accuracy that is sufficient to test this sector of physics at low energy with light nuclei.

6.6 Concluding Remarks

To conclude we shall address a fundamental aspect related to the concept of the ''potential function'', which appears in the usual discussions of tunnelling. Indeed, at first sight it may seem that the concept of ''tunnelling'' necessarily involves the existence of such a potential function. A closer look shows, however, that things are not quite as simple. We shall start here by considering tunnelling within the quasiadiabatic channel reaction path Hamiltonian and ''quasiadiabatic above-barrier tunnelling''. In vibrationally excited states of HOOH the wave functions show a tunnelling sublevel structure and tunnelling wave packet dynamics as given by the effective one-dimensional quasiadiabatic channel potential, although their energy is high above the barrier in the multidimensional Born–Oppenheimer surface.

One might then be tempted to say that it is not a ''true'' tunnelling process, as it results from an approximate model. However, the ''exact'' six-dimensional vibration-tunnelling calculation on the complete hypersurface shows about the same level structure and wave packet dynamics as the approximate calculations, and therefore one must conclude that the full quantum dynamics shows ''tunnelling behavior'' even above the barrier. This has led us to introduce the concept of quasiadiabatic channel above barrier tunnelling of importance also in other contexts.[196]

It is furthermore also true that the tunnelling sublevel structure and dynamics at energies below the six-dimensional saddle point result from an approximation. Without the Born–Oppenheimer approximation the ''Born–Oppenheimer potential barriers and saddle points'' disappear. If one treats hydrogen peroxide or other molecules with Born–Oppenheimer barriers ''exactly'' by means of quantum dynamics of a collection of the electrons and nuclei in the molecule, the ''true'' potential arises in essence from the Coulomb interaction of these particles in a very high dimensional space (for instance 60 dimensions for HOOH). However, even then, without any Born–Oppenheimer barriers to tunnel through, the ''exact'' quantum dynamics will show very much the same sublevel structure and tunnelling dynamics as is described by the approximate theory and confirmed by experiment. This suggests a new definition of quantum tunnelling dynamics that does not depend on the concept of potential barriers, as we have pointed out already in the context of the definition of the ''molecular symmetry group'' of non-rigid molecules.[27,195,198] While Longuet-Higgins has, indeed, motivated this group by the existence of high Born–Oppenheimer potential barriers separating symmetrically equivalent isomers and thereby generating systematically degenerate level structures,[197] we pointed out that in a rigorous discussion the symmetry groups should not be defined by an approximation but rather by the induced representation corresponding to the degenerate sublevels, which one can define from an exact theory without any approximation and also by experiment (ref. 27, 195, 198 and references therein). When the perfect degeneracy is lifted by tunnelling leading to observable tunnelling splittings, one can consider this effect, then, as the breaking of an approximate symmetry without having to refer to tunnelling through potential barriers from the Born–Oppenheimer approximation. Thus, the tunnel effect in molecules can be understood as a quantum dynamical phenomenon without making reference to approximate concepts such as Born–Oppenheimer potential hypersurfaces. One can say, however, that the Born–Oppenheimer approximation, and also the quasiadiabatic channel reaction path Hamiltonian with their effective potentials, provide us with simple models[190] that allow us, in the first place, to qualitatively understand the phenomena and, in the second place, to compute the phenomena approximately without too much effort (see also the general discussion by Roald Hoffmann[191] on qualitative understanding *versus* computation). The discussion can be continued similarly at an even deeper level: from the standard model of particle physics we understand even the Coulomb potential as not being a ''fundamental

preexisting'' potential but rather as arising from photons as field particles mediating the electromagnetic interaction, as discussed in Section 6.2. Similarly the parity-violating interaction leading to the slight asymmetry effect in the effective potential, as illustrated in Figures 6.6 and 6.7 arises from the Z-bosons as field particles mediating the weak interaction between electrons and nuclei (or protons, neutrons, quarks, *etc.*). The small effective ''parity-violating potential'' (really an extra effective potential hypersurface that is antisymmetric with respect to inversion and should not at all be interpreted as a ''Born–Oppenheimer hypersurface'') arises from an approximation in carrying out the computation in electroweak quantum chemistry.[27] While there would be no need to make the approximation, it nevertheless corresponds to a useful model that allows us to understand the small symmetry violation and to practically compute it with feasible effort. Conceptually, however, exact tunnelling dynamics in this effective asymmetric potential should be understood on the basis of the quantum sublevel structure arising from the symmetry breaking removal of a degeneracy, which can be observed by experiment or could also be derived from an exact theory without making any reference to the parity-violating potential hypersurface, nor to the Born–Oppenheimer surface for that matter.

A brief note is also useful concerning the role of relativistic effects. As is well known, these are important for the dynamics of electron motion whenever the heavier elements are involved in the molecules considered. These effects can be calculated by relativistic quantum chemistry[192,199,205] and can lead, indeed, to dramatic changes in the effective Born–Oppenheimer potential barriers for tunnelling. Once these effects are included, the tunnelling motion of atoms and molecules can be computed and understood in very much the same way using the Schrödinger equation, as discussed for non-relativistic potentials. If the molecules move at relativistic speeds, one has to consider the changes in the definition of time that is then to be measured by an atomic clock moving at relativistic speed.[42,110,204] Indeed, molecular tunnelling systems such as ammonia can be, and have been, used as molecular clocks, and one has the well-understood (and in fact experimentally observed) relativistic effects, such as an atomic and molecular ''twin paradox'' discussed by Einstein.[193] Further considerations arise when considering violations of time-reversal symmetry and possibly a hypothetical violation of CPT symmetry[42,178,200–204,206] and we refer to ref. 27, 157 and 158, where one can also find a discussion of fundamental aspects of the definition of time and of the ''42 open problems'', some of which are related to tunnelling.

Acknowledgements

We gratefully acknowledge support, help from and discussions with Ziqiu Chen, Csabá Fabri, Karen Keppler, Roberto Marquardt, Frédéric Merkt, Eduard Miloglyadov, Robert Prentner, Jürgen Stohner, Martin Willeke, and Gunther Wichmann as well as financial support from ETH Zürich, the laboratory of Physical Chemistry and an Advanced Grant of the European

Research Council ERC, as well as the COST project MOLIM. This publication is based on a lecture (San Diego, ACS August 2019) and dedicated to HF Schaefer III on the occasion of his 75th birthday.

References

1. F. Hund, *Z. Phys.*, 1927, **43**, 788.
2. F. Hund, *Z. Phys.*, 1927, **43**, 805.
3. F. Hund, *Z. Phys.*, 1927, **40**, 742.
4. W. Heisenberg, *Z. Physik*, 1925, **33**, 879.
5. W. Heisenberg, *Die Physikalischen Prinzipien der Quantentheorie*, Hirzel Verlag, Leipzig, 1980.
6. P. A. M. Dirac, *The Principles of Quantum Mechanics*, 4th edn, Clarendon Press, Oxford, 1958.
7. E. Schrödinger, *Ann. Phys.*, 1926, **81**, 109.
8. E. Schrödinger, *Ann. Phys.*, 1926, **79**, 361.
9. E. Schrödinger, *Ann. Phys.*, 1926, **79**, 489.
10. E. Schrödinger, *Ann. Phys.*, 1926, **80**, 437.
11. E. Schrödinger, *Naturwissenschaften*, 1926, **14**, 664.
12. M. Quack, *Bunsenmagazin*, 2012, **14**, 181.
13. W. J. Moore, *Schrödinger, Life and Thought*, Cambridge Univ. Press, Cambridge, 1989, p. 195.
14. G. Seyfang and M. Quack, *Nachr. Chemie*, 2017, **66**, 307.
15. M. Quack and G. Seyfang, Atomic and molecular tunnelling processes in chemistry, Chapter 7 in *Time Dependent Quantum Dynamics and Spectroscopy*, ed. R. Marquardt and M. Quack, Elsevier, Amsterdam, 2020.
16. J. Kästner and S. Kozuch, *Quantum Mechanical Tunneling*, Royal Society of Chemistry, 2020.
17. R. K. Allemann and N. S. Scrutton, *Quantum Tunneling in Enzyme-catalysed Reactions*. RSC Publishing, Cambridge, 2009.
18. B. P. Bell, *The Tunnel Effect in Chemistry*, Chapman and Hall, London, 1980.
19. G. Herzberg, *Molecular Spectra and Molecular Structure: II. Infrared and Raman Spectra*, Van Nostrand, New York, 1943.
20. G. Herzberg, *Molecular Spectra and Molecular Structure: III. Electronic Spectra and Electronic Structure of Polyatomic Molecules*, Van Nostrand, New York, 1966.
21. M. Quack and F. Merkt, *Handbook of High-Resolution Spectroscopy*, John Wiley, Chichester, New York, 2011.
22. T. D. Lee and C. D. Yang, *Phys. Rev.*, 1956, **104**, 254.
23. C. S. Wu, E. Ambler, R. W. Hayward, D. D. Hoppes and R. P. Hudson, *Phys. Rev.*, 1957, **105**, 1413.
24. J. I. Friedman and V. Telegdi, *Phys. Rev.*, 1957, **105**, 1681.
25. H. Schopper, *Phil. Mag.*, 1957, **2**, 710.
26. R. L. Garwin, L. M. Lederman and M. Weinrich, *Phys. Rev.*, 1957, **105**, 1415.

27. M. Quack, Fundamental symmetries and symmetry violations from high resolution spectroscopy, in *Handbook of High Resolution Spectroscopy*, ed. M. Quack and F. Merkt, Wiley, Chichester, New York, 2011, vol. 1, ch. 18, pp. 659.
28. *Symmetrie und Asymmetrie in Wissenschaft und Kunst, Nova Acta Leopoldina NF*, ed. M. Quack and J. Hacker, 2016, vol. 127, No. 412, p. 7 (preface to book with a total of 275 pages and contributions by several authors in English and German).
29. M. Quack, Electroweak quantum chemistry and the dynamics of parity violation in chiral molecules, in *Modelling Molecular Structure and Reactivity in Biological Systems, Proc. 7th WATOC Congress, Cape Town January 2005*, ed. K. J. Naidoo, J. Brady, M. J. Field, J. Gao and M. Hann, Royal Society of Chemistry, Cambridge, 2006, pp. 3–38.
30. M. Quack, J. Stohner and M. Willeke, *Ann. Rev. Phys. Chem.*, 2008, **59**, 741.
31. M. Quack, Molecular Parity Violation and Chirality: The Asymmetry of Life and the Symmetry Violations of Physics, in *Quantum Systems in Chemistry and Physics: Progress in Methods and Applications, Proceedings of QSCP XVI, Kanazawa 11 to 17 September 2011'', Series Title: ''Progress in Theoretical Chemistry and Physics*, ed. K. Nishikawa, J. Maruani, E. Brändas, G. Delgado-Barrio and P. P. Piecuch, Springer Verlag , 2012, ch. 3, pp. 47–76.
32. M. Quack, *Adv. Chem. Phys.*, 2014, **157**, 249.
33. A. Bakasov, T. K. Ha and M. Quack, Ab initio calculation of molecular energies including parity-violating interactions, in *Chemical Evolution, Physics of the Origin and Evolution of Life, Proc. of the 4th Trieste Conference (1995)*, ed. J. Chela-Flores and F. Raulin, Kluwer Academic Publishers, Dordrecht, 1996, p. 287.
34. A. Bakasov, T. K. Ha and M. Quack, *J. Chem. Phys.*, 1998, **109**, 7263.
35. R. Berger and M. Quack, *J. Chem. Phys.*, 2000, **112**, 3148.
36. M. Quack, *Angew. Chem., Int. Ed. Engl.*, 2002, **41**, 4618–4630.
37. P. A. M. Dirac, *Proc. R. Soc. London, A*, 1929, **123**, 714.
38. CERN, Webseite http://doc.cern.ch//archive/electronic/cern/others/PHO/photodi/9809005.jpeg, Bildnummer CERN AC_Z04_V25/B/1992.
39. J. H. van't Hoff, *La chimie dans l'espace*, ed. B. M. Bazendijk, Rotterdam, reprinted in ed. and C. Bourgeois, Sur la dissymétrie moléculaire, Coll. Epistème, Paris, 1986, 1887.
40. M. Quack and J. Stohner, *Phys. Rev. Lett.*, 2000, **84**, 3807.
41. M. Quack, *Angew. Chem., Int. Ed. Engl.*, 1989, **28**, 571. *Angew. Chem.*, 1989, **101**, 588.
42. M. Quack, Time and time reversal symmetry in quantum chemical kinetics, in *Fundamental World of Quantum Chemistry, a Tribute to the Memory of Per Olof Löwdin*, ed. E. J. Brändas and E. S. Kryachko, Kluver Publ., Dordrecht, 2004, vol. 3, pp. 423.
43. S. L. Glashow, *Nucl. Phys.*, 1961, **22**, 579.
44. S. Weinberg, *Phys. Rev. Letters*, 1967, **19**, 1264.

45. A. Salam, *Proceedings of the 8th Nobel Symposium*, Almkvist und Wiksell, Stockholm, 1968, p. 367.
46. M. J. G. Veltman, *Rev. Mod. Phys.*, 2000, **72**, 341.
47. G. 't Hooft, *Rev. Mod. Phys.*, 2000, **72**, 333.
48. Y. Yamagata, *J. Theor. Biol.*, 1966, **11**, 495.
49. A. S. Garay and P. Hrasko, *J. Mol. Evol.*, 1975, **6**, 77.
50. D. W. Rein, *J. Mol. Evol.*, 1974, **4**, 15.
51. V. S. Letokhov, *Phys. Lett. A*, 1975, **53**, 275.
52. O. N. Kompanets, A. R. Kukudzhanov, V. S. Letokhov and L. L. Gervits, *Opt. Commun.*, 1976, **19**, 414.
53. E. Arimondo, P. Glorieux and T. Oka, *Opt. Commun.*, 1977, **23**, 369.
54. L. Keszthelyi, *Phys. Lett. A*, 1977, **64**, 287.
55. L. Keszthelyi, *Orig. Life Evol. Biosph.*, 1977, **8**, 299.
56. B. Y. Zeldovich, D. B. Saakyan and I. I. Sobelman, *JETP Lett.*, 1977, **25**, 94.
57. R. A. Harris and L. Stodolsky, *Phys. Lett. B*, 1978, **78**, 313.
58. D. W. Rein, R. A. Hegström and P. G. H. Sandars, *Phys. Lett. A*, 1979, **71**, 499.
59. R. A. Hegström, D. W. Rein and P. G. H. Sandars, *J. Chem. Phys.*, 1980, **73**, 2329.
60. S. F. Mason and G. E. Tranter, *J. Chem. Soc. Chem. Comm*, 1983, 117.
61. S. F. Mason and G. E. Tranter, *Chem. Phys. Lett.*, 1983, **94**, 34.
62. S. F. Mason and G. E. Tranter, *Mol. Phys.*, 1984, **53**, 1091.
63. S. F. Mason, *Nature*, 1984, **311**, 19.
64. G. E. Tranter, *Mol. Phys.*, 1985, **56**, 825.
65. G. E. Tranter, *Chem. Phys. Lett.*, 1985, **121**, 339.
66. G. E. Tranter, *Chem. Phys. Lett.*, 1985, **115**, 286.
67. G. E. Tranter, *Nature*, 1985, **318**, 172.
68. A. L. Barra, J. B. Robert and L. Wiesenfeld, *Phys. Lett. A*, 1986, **115**, 443.
69. A. L. Barra, J. B. Robert and L. Wiesenfeld, *BioSystems*, 1987, **20**, 57.
70. D. K. Kondepudi, *BioSystems*, 1987, **20**, 75.
71. A. J. Macdermott, G. E. Tranter and S. B. Indoe, *Chem. Phys. Lett.*, 1987, **135**, 159.
72. A. L. Barra, J. B. Robert and L. Wiesenfeld, *Europhys. Lett.*, 1988, **5**, 217.
73. L. Wiesenfeld, *Mol. Phys.*, 1988, **64**, 739.
74. P. Jungwirth, L. Skala and R. Zahradnik, *Chem. Phys. Lett.*, 1989, **161**, 502.
75. A. J. Macdermott and G. E. Tranter, *Chem. Phys. Lett.*, 1989, **163**, 1.
76. A. J. Macdermott and G. E. Tranter, *Croat. Chem. Acta*, 1989, **62**, 165.
77. O. Kikuchi and H. Wang, *Bull. Chem. Soc. Jpn.*, 1990, **63**, 2751.
78. O. Kikuchi, H. Wang, T. Nakano and K. Morihashi, *Theochem.-J. Mol. Struct.*, 1990, **64**, 301.
79. J. Chela-Flores, *Chirality*, 1991, **3**, 389.
80. A. Salam, *J. Mol. Evol.*, 1991, **33**, 105.
81. A. Salam, *Phys. Lett. B*, 1992, **288**, 153.
82. O. Kikuchi and H. Kiyonaga, *Theochem-J. Mol. Struct.*, 1994, **118**, 271.

83. A. Bakasov, T. K. Ha and M. Quack, *Chimia*, 1997, **51**, 559.
84. A. Bakasov and M. Quack, *Chem. Phys. Lett.*, 1999, **303**, 547.
85. R. Berger and M. Quack, *Proc. 37th IUPAC Congress*, Berlin, 1999, vol. 2, p. 518.
86. P. Lazzeretti and R. Zanasi, *Chem. Phys. Lett.*, 1997, **279**, 349.
87. R. Zanasi and P. Lazzeretti, *Chem. Phys. Lett.*, 1998, **286**, 240.
88. J. K. Laerdahl and P. Schwerdtfeger, *Phys. Rev. A*, 1999, **60**, 4439.
89. M. Gottselig, D. Luckhaus, M. Quack, J. Stohner and M. Willeke, *Helv. Chim. Acta*, 2001, **84**, 1846.
90. R. Berger, M. Gottselig, M. Quack and M. Willeke, *Angew. Chem., Int. Ed.*, 2001, **40**, 4195, (*Angew. Chem.*, 2001, **113**, 4342).
91. M. Quack and J. Stohner, *Z. Phys. Chem.*, 2000, **214**, 675. *Proc. 12th Symp. on Atomic and Surface Physics and related Topics*, ed. D. Bassi and P. Tosi, Folgaria, Trento, 2000, PR-11, pp. 1–4.
92. R. Berger and M. Quack, *ChemPhysChem*, 2000, **1**, 57.
93. R. Berger, M. Quack and G. S. Tschumper, *Helv. Chim. Acta*, 2000, **83**, 1919.
94. J. K. Laerdahl, P. Schwerdtfeger and H. M. Quiney, *Phys. Rev. Lett.*, 2000, **84**, 3811.
95. J. K. Laerdahl, R. Wesendrup and P. Schwerdtfeger, *ChemPhysChem*, 2000, **1**, 60.
96. A. C. Hennum, T. Helgaker and W. Klopper, *Chem. Phys. Lett.*, 2002, **354**, 274.
97. M. Quack and J. Stohner, *Chirality*, 2001, **13**, 745.
98. A. Beil, D. Luckhaus, R. Marquardt and M. Quack, *Faraday Discuss.*, 1994, **99**, 49.
99. A. Bauder, A. Beil, D. Luckhaus, F. Müller and M. Quack, *J. Chem. Phys.*, 1997, **106**, 7558.
100. H. Hollenstein, D. Luckhaus, J. Pochert, M. Quack and G. Seyfang, *Angew. Chem., Int. Ed. Engl.*, 1997, **36**, 140, (*Angew. Chem.*, **109**, 136).
101. C. Daussy, Premier test de très haute précision de violation de la parité dans le spectre de la molécule chirale CHFClBr, Thèse, Université Paris 13, Villetaneuse, Paris Nord, 1999.
102. C. Daussy, T. Marrel, A. Amy-Klein, C. T. Nguyen, C. J. Bordé and C. Chardonnet, *Phys. Rev. Lett.*, 1999, **83**, 1554.
103. J. Crassous and A. Collet, *Enantiomer*, 2000, **5**, 429.
104. M. J. M. Pepper, I. Shavitt, P. V. R. Schleyer, M. N. Glukhovtsev, R. Janoschek and M. Quack, *J. Comput. Chem.*, 1995, **16**, 207.
105. M. Quack, *Faraday Discuss.*, 1994, 389.
106. R. Berger, *Phys. Chem. Chem. Phys.*, 2003, **5**, 12.
107. A. S. Lahamer, S. M. Mahurin, R. N. Compton, D. House, J. K. Laerdahl, M. Lein and P. Schwerdtfeger, *Phys. Rev. Lett.*, 2000, **85**, 4470.
108. H. Buschmann, R. Thede and D. Heller, *Angew. Chem., Int. Ed.*, 2000, **39**, 4033.
109. P. Frank, W. Bonner and R. N. Zare, in *Chemistry for the 21st Century*, ed. E. Keinan and I. Schechter, Wiley-VCH, Weinheim, 2001, ch. 11, p. 175.

110. M. Quack, Zeit und Zeitumkehrsymmetrie in der molekularen Kinetik. Schriftliche Fassung des Vortrages am 7. Symposium der Deutschen Akademien der Wissenschaften, Berlin-Brandenburgische Akademie der Wissenschaften Berlin, Zeithorizonte in der Wissenschaften, 31.10. und 1.11.2002, ed. D. Simon, De Gruyter, Berlin, 2004, p. 125.
111. M. Quack and J. Stohner, *Chimia*, 2005, **59**, 530.
112. H. F. Schaefer III, *Quantum Chemistry. The Development of ab initio Methods in Molecular Electronic Structure Theory*, Clarendon Press, Oxford, 1984.
113. H. F. Schaefer, *Chimia*, 1989, **43**, 1.
114. W. G. Richards, *Nature*, 1979, **278**, 507.
115. C. F. Bender and H. F. Schaefer III, *J. Am. Chem. Soc.*, 1970, **92**, 4984.
116. C. F. Bender and H. F. Schaefer III, *J. Am. Chem. Soc.*, 1972, **94**, 6888.
117. A. G. Császár, C. Fábri, T. Szidarovszky, E. Mátyus, T. Furtenbacher and G. Czakó, *PhysChemChemPhys*, 2012, **14**, 1085.
118. N. N. Bogoljubov and D. V. Shirkov, *Quantum Fields, Benjamin/Cummings, Reading, Massachusetts etc.*, 1983.
119. N. N. Bogoljubov and D. V. Shirkov, *Introduction to the Theory of Quantized Fields*, Wiley, New York *a.o.*, 1980.
120. A. Bakasov, T. K. Ha and M. Quack, Parity-violating potentials for molecules and clusters, in *Proceedings of the Symposium on Atomic and Surface Physics and Related Topics, SASP 98, Going/Kitzbühel, Austria*, ed. A. Hansel and W. Lindinger, Institut für Ionenphysik der Universität Innsbruck, 1998, p. 4.
121. M. A. Bouchiat and C. Bouchiat, *J. Phys.*, 1974, **35**, 899.
122. M. A. Bouchiat and C. Bouchiat, *J. Phys.*, 1975, **36**, 493.
123. J. Linderberg and Y. Öhrn, *Propagators in Quantum Chemistry*, Academic Press, London, 1973.
124. O. Vahtras, H. Agren, P. Jorgensen, H. J. A. Jensen, T. Helgaker and J. Olsen, *J. Chem. Phys.*, 1992, **96**, 2118.
125. R. Berger and C. van Wüllen, *J. Chem. Phys.*, 2005, **122**, 134316.
126. P. Schwerdtfeger, T. Saue, J. N. P. van Stralen and L. Visscher, *Phys. Rev. A*, 2005, **71**, 012103.
127. M. Quack and J. Stohner, *J. Chem. Phys.*, 2003, **119**, 11228.
128. A. Bakasov, R. Berger, T. K. Ha and M. Quack, *Int. J. Quantum Chem.*, 2004, **99**, 393.
129. M. Quack, *Annu. Rev. Phys. Chem.*, 1990, **41**, 839.
130. M. Quack, Molecular femtosecond quantum dynamics between less than yoctoseconds and more than days: Experiment and theory in Femtosecond Chemistry, in *Proc. Berlin Conf. Femtosecond Chemistry, Berlin (March 1993)*, ed. J. Manz and L. Woeste, Verlag Chemie, Weinheim, 1995, ch. 27, p. 781.
131. B. Kuhn, T. R. Rizzo, D. Luckhaus, M. Quack and M. A. Suhm, *J. Chem. Phys.*, 1999, **111**, 2565.
132. B. Fehrensen, D. Luckhaus and M. Quack, *Chem. Phys. Lett.*, 1999, **300**, 312.

133. D. Luckhaus and M. Quack, Gas Phase Kinetics Studies, in *Encyclopedia of Chemical Physics and Physical Chemistry*, ed. J. H. Moore and N. Spencer, IOP Publishing, Bristol, 2001, vol. 2, (Methods), ch. B. 2.5, p. 1871.
134. R. Berger, M. Quack, A. Sieben and M. Willeke, *Helv. Chim. Acta*, 2003, **86**, 4048.
135. M. Gottselig, M. Quack, J. Stohner and M. Willeke, *Int. J. Mass Spectrom.*, 2004, **233**, 373.
136. B. Fehrensen, D. Luckhaus and M. Quack, *Z. Phys. Chem.*, 1999, **209**, 1.
137. W. B. Olson, R. H. Hunt, B. W. Young, A. G. Maki and J. W. Brault, *J. Mol. Spectrosc.*, 1988, **127**, 12.
138. M. Quack and M. Willeke, *Helv. Chim. Acta*, 2003, **86**, 1641.
139. M. Quack, *Chimia*, 2001, **55**, 753.
140. M. Quack, *Philos. Trans. Roy. Soc. London*, 1990, **A 332**, 203.
141. M. Gottselig and M. Quack, *J. Chem. Phys.*, 2005, **123**, 84305.
142. J. K. Laerdahl and P. Schwerdtfeger, *Phys. Rev. A*, 1999, **60**, 4439.
143. L. Horný and M. Quack, *Faraday Discuss.*, 2011, **150**, 152.
144. P. Lazzeretti, R. Zanasi and F. Faglioni, *Phys Rev E*, 1999, **60**, 871.
145. R. Berger, Parity-violation effects in molecules, in *Relativistic Electronic Structure Theory, Vol. Part 2*, ed. P. Schwerdtfeger, Elsevier, Amsterdam, 2004, ch. 4, pp. 188–288.
146. R. Berger, M. Quack and J. Stohner, *Angew. Chem., Int. Ed.*, 2001, **40**, 1667, (*Angew. Chem.*, **113**, 1716).
147. E. Fermi, *Z. Physik*, 1934, **89**, 522.
148. F. Hobi, R. Berger and J. Stohner, *Mol. Phys.*, 2013, **111**, 2345.
149. M. Quack, *Chem. Phys. Lett.*, 1986, **132**, 147.
150. M. Quack and M. Willeke, *J. Phys. Chem. A*, 2006, **110**, 3338.
151. L. Horný and M. Quack, *Mol. Phys.*, 2015, **113**, 1768.
152. R. Prentner, M. Quack, J. Stohner and M. Willeke, *J. Phys. Chem. A*, 2015, **119**, 12805.
153. R. Berger, *J. Chem. Phys.*, 2008, **129**, 154105.
154. J. N. P. van Stralen, L. Visscher, C. V. Larsen and H. J. A. Jensen, *Chem. Phys.*, 2005, **311**, 81.
155. R. Berger, N. Langermann and C. vanWüllen, *Phys. Rev.*, 2005, **A 71**, 042105.
156. J. Thyssen, J. K. Laerdahl and P. Schwerdtfeger, *Phys. Rev. Lett.*, 2000, **85**, 3105.
157. M. Quack, *Die Symmetrie von Zeit und Raum und ihre Verletzung in molekularen Prozessen in Jahrbuch 1990-1992 der Akademie der Wissenschaften zu Berlin, W. de Gruyter*, Verlag, Berlin, 1993, pp. 467, (printed version of the 8th public academy lecture, Berlin 4.10.1990); there exists also a slightly changed English version: M. Quack, The symmetries of time and space and their violation in chiral molecules and molecular processes, pp. 172, in *Conceptual Tools for Understanding Nature. Proc. 2nd Int. Symp. of Science and Epistemology Seminar, Trieste April 1993*, ed. G. Costa, G. Calucci and M. Giorgi, World Scientific Publ., Singapore, 1995.

158. M. Quack, *Faraday Disc*, 2011, **150**, 533.
159. E. R. Cohen, T. Cvitas, J. G. Frey, B. Holmström, K. Kuchitsu, R. Marquardt, I. Mills, F. Pavese, M. Quack, J. Stohner, H. L. Strauss, M. Takami and A. Thor, *Quantities, Units and Symbols in Physical Chemistry*, 3rd edn, 2007.
160. R. Berger, G. Laubender, M. Quack, A. Sieben, J. Stohner and M. Willeke, *Angew. Chem.*, 2005, **117**, 3689, (*Angew. Chem., Int. Ed. (Engl.)*, 2005, **44**, 3623).
161. M. Quack, *Nova Acta Leopoldina*, 1999, **81**(Neue Folge (No. 314)), 137.
162. S. Albert, I. Bolotova, Z. Chen, C. Fábri, L. Horný, M. Quack, G. Seyfang and D. Zindel, *Phys. Chem. Chem. Phys.*, 2016, **18**, 21976.
163. S. Albert, K. Keppler, V. Boudon, P. Lerch and M. Quack, *J. Mol. Spect*, 2017, **337**, 105.
164. S. Albert, I. Bolotova, Z. Chen, C. Fábri, M. Quack, G. Seyfang and D. Zindel, *Phys. Chem. Chem. Phys.*, 2017, **19**, 11738.
165. C. Fábri, L. Horný and M. Quack, *ChemPhysChem*, 2015, **16**, 3584.
166. S. Albert, F. Arn, I. Bolotova, Z. Chen, C. Fábri, G. Grassi, P. Lerch, M. Quack, G. Seyfang, A. Wokaun and D. Zindel, *J. Phys. Chem. Lett.*, 2016, **7**, 3847.
167. S. Albert, Z. Chen, K. Keppler, P. Lerch, M. Quack, V. Schurig and O. Trapp, *Phys. Chem. Chem. Phys.*, 2019, **21**, 3669.
168. S. Albert, P. Lerch, K. Keppler and M. Quack, *Proceedings of the 20th Symposium on Atomic, Cluster and Surface Physics 2016 (SASP 2016), Davos, Switzerland, 7 to 12 February 2016*, ed. J. Stohner and Ch. Yeretzian, Innsbruck University Press (IUP), Innsbruck, 2016, pp. 165–168.
169. B. Fehrensen, D. Luckhaus and M. Quack, *Chem. Phys.*, 2007, **338**, 90.
170. M. Hippler, E. Miloglyadov, M. Quack and G. Seyfang, Mass and isotope selective infrared spectroscopy, in *Handbook of High Resolution Spectroscopy*, ed. M. Quack and F. Merkt, Wiley, Chichester, New York, 2011, vol. 2, ch. 28, pp. 1069.
171. S. Albert, P. Lerch and M. Quack, *Proceedings of the 20th Symposium on Atomic, Cluster and Surface Physics 2016 (SASP 2016), Davos, Switzerland, 7 to 12* February 2016, ed. J. Stohner and Ch. Yeretzian, Innsbruck University Press (IUP), Innsbruck, 2016, p. 169.
172. C. Fábri, R. Marquardt, A. Császár and M. Quack, *J. Chem. Phys.*, 2019, **150**, 014102.
173. M. Gottselig, M. Quack and M. Willeke, *Israel J. Chem.*, 2003, **43**, 353.
174. S. K. Tokunaga, C. Stoeffler, F. Auguste, A. Shelkovnikov, C. Daussy, A. Amy-Klein, C. Chardonnet and B. Darquié, *Mol. Phys.*, 2013, **111**, 2363.
175. M. Schnell and J. Küpper, *Farad. Discuss. Chem. Soc*, 2011, **150**, 33.
176. M. Quack, *Farad. Discuss. Chem. Soc*, 2011, **150**, 123.
177. R. Marquardt, M. Quack, J. Thanopulos and D. Luckhaus, *J. Chem. Phys.*, 2003, **118**, 643.
178. M. Quack, *Chimia*, 2003, **57**, 147.
179. S. Albert, P. Lerch, R. Prentner and M. Quack, *Angew. Chem. Intl. Ed.*, 2013, **52**, 346, (*Angew. Chem.*, **125**, 364).

180. J. K. G. Watson, in *Vibrational Spectra and Structure*, ed. J. R. Durig, Elsevier, Amsterdam, vol. 6, 1978, p. 1.
181. P. Dietiker, M. Miloglyadov, M. Quack, A. Schneider and G. Seyfang, *J. Chem. Phys.*, 2015, **143**, 244305.
182. E. Miloglyadov, M. Quack, G. Seyfang, G. Wichmann, Chapter A.2.3 Precision Experiments for Parity Violation in Chiral Molecules: the Role of STIRAP 11–13, 51–52 in K. Bergmann, H.-C. Nägerl, C. Panda, G. Gabrielse, E. Miloglyadov, M. Quack, G. Seyfang, G. Wichmann, S. Ospelkaus, A. Kuhn, S. Longhi, A. Szameit, P. Pirro, B. Hillebrands, X.-F. Zhu, J. Zhu, M. Drewsen, W. K. Hensinger, S. Weidt, T. Halfmann, H.-L. Wang, G. Sorin Paraoanu, N. V. Vitanov, J. Mompart, T. Busch, T. J. Barnum, D. D. Grimes, R. W. Field, M. G. Raizen, E. Narevicius, M. Auzinsh, D. Budker, A. Pálffy, C. H. Keitel, *J. Phys. B: At., Mol. Opt. Phys.* 2019, **52**, 202001.
183. S. Albert, Z. Chen, K. Keppler, C. Manca Tanner, M. Quack, V. Schurig, J. Stohner and O. Trapp, *Chimia*, 2019, **73**, 615, and to be published.
184. A. Garg, *Am. J. Phys.*, 2000, **68**, 430.
185. D. Luckhaus and M. Quack, *Mol. Phys.*, 1989, **68**, 745.
186. C. Fábri, S. Albert, Z. Chen, R. Prentner and M. Quack, *Phys. Chem. Chem. Phys.*, 2018, **20**, 7387.
187. S. Albert, Z. Chen, C. Fábri, P. Lerch, R. Prentner and M. Quack, *Mol. Phys.*, 2016, **114**, 2751.
188. J. Smydke, C. Fábri, C. Sarka and A. Császár, *Phys. Chem. Chem. Phys.*, 2019, **21**, 3453.
189. *Molecular Switches*, ed. B. L. Feringa and W. R. Browne, Wiley-VCH Verlag GmbH & Co. KGaA, 2nd edn, 2011.
190. M. Quack, *European Review*, 2014, **22**, S 50.
191. R. Hoffmann, *J. Mol. Struct.*, 1998, **424**, 1.
192. M. Reiher and A. Wolf, *Relativistic Quantum Chemistry: The Fundamental Theory of Molecular Science*, 1st edn, Wiley-VCH, Weinheim, 2009.
193. A. Einstein, *Grundzüge der Relativitätstheorie*, Vieweg, Braunschweig, 1922.
194. U. Gaubatz, P. Rudecki, S. Schieman and K. Bergman, *J. Chem. Phys.*, 1990, **92**, 5363.
195. M. Quack, *J. Chem. Phys.*, 1985, **82**, 3277.
196. M. Quack and M. Suhm, *J. Chem. Phys.*, 1991, **95**, 28.
197. H. C. Longuet-Higgins, *Mol. Phys.*, 1963, **6**, 445.
198. M. Quack, *Mol. Phys.*, 1977, **34**, 477.
199. R. Mastalerz and M. Reiher, Relativsitic Electronic Structure Theory for Molecular Spectroscopy, in *Handbook of High Resolution Spectroscopy*, ed. M. Quack and F. Merkt, Wiley, Chichester, 2011, vol. 1, p. 405.
200. M. Quack, *Chem. Phys. Lett.*, 1994, **231**, 421.
201. M. Quack, *J. Mol. Struct.*, 1993, **292**, 171.
202. G. Gabrielse, *Nova Acta Leopoldina, NF*, 2016, **127**(412), 91, (see ref. 28).
203. H. Fritsch, *Nova Acta Leopoldina, NF*, 2016, **127**(412), 75, (see ref. 28).
204. M. Quack, *Nova Acta Leopoldina, NF*, 2016, **127**(412), 119, (see ref. 28).
205. P. Pyykkö, *Chem. Rev.*, 2012, **112**, 371.

206. ALPHA Collaboration, *Nature*, 2020, **578**, 375, (M. Ahmadi, *et al.*).
207. B. Fehrensen, D. Luckhaus and M. Quack, *Z. Phys. Chem.*, 1999, **300**, 312.
208. W. H. Miller, N. C. Handy and J. E. Adams, *J. Chem. Phys.*, 1980, **72**, 99.
209. M. Quack and J. Troe, *Ber. Bunsenges. Phys. Chem.*, 1974, **78**, 240.
210. M. Quack and J. Troe, Statistical Adiabatic Channel Models, in *Encyclopedia of Computational Chemistry*, ed. P. von Ragué Schleyer, N. Allinger, T. Clark, J. Gasteiger, P. A. Kollman, H. F. Schaefer III and P. R. Schreiner, John Wiley and Sons, 1998, vol. 4, p. 2708.
211. M. Quack, *J. Chem. Phys.*, 1978, **69**, 1282.
212. H. Feldmann, D. Kella, E. Malkin, E. Miklazky, Z. Vager, J. Zajfman and R. Naaman, *J. Chem. Soc. Farad. Trans*, 1990, **86**, 2469.
213. P. Herwig, K. Zawatzky, M. Grieser, O. Heber, B. Jordon-Thaden, C. Krantz, O. Novotny, R. Repnow, V. Schurig, D. Schwalm, Z. Vager, A. Wolf, O. Trapp and H. Kreckel, *Science*, 2013, **342**, 1084.
214. M. Pitzer, R. Berger, J. Stohner, R. Dörner and M. Schöffler, *Chimia*, 2018, **72**, 384.
215. L. Barron, *Molecular Light Scattering and Optical Activity*, 2nd edn, Cambridge University Press, 2004.
216. L. Wilhelmy, *Poggendorfs Ann.*, 1850, **81**, 413 and 419.
217. M. Quack, *Adv. Chem. Phys.*, 2014, **157**, 97.
218. L. Hoddeson, L. Brown, M. Riordan and M. Dresden, *The Rise of the Standard Model: A History of Particle Physics from 1964 to 1979*, Cambridge University Press, 1997.
219. *60 Years of CERN, Experiments and Discoveries*, ed. H. Schopper and L. Di Lella, World Scientific, Singapore, 2015.
220. S. C. Bennet and C. E. Wieman, *Phys. Rev. Lett.*, 1999, **82**, 2484.
221. R. Berger and J. Stohner, *WIREs Comp. Mol. Sci*, 2019, **9**(3), e1396.
222. M. K. Kozlov and L. N. Labzowski, *J. Phys. B: At., Mol. Opt. Phys.*, 1995, **28**, 1933.
223. A. Császár and C. Fábri, From Tunnelling Control to Controlling Tunnelling, in *Quantum Mechanical Tunneling*, ed. J. Kästner and S. Kozuch, Royal Society of Chemistry, 2020, pp. 146–166.
224. A. Cournol, M. Manceau, M. Pierens, L. Lecordier, D. B. A. Tran, R. Santagata, B. Argence, A. Goncharov, O. Lopez, M. Abgrall, Y. Le Coq, R. Le Targat, H. Alvarez Martinez, W. L. Lee, D. Xu, P. E. Pottie, R. J. Hendricks, T. E. Wall, J. M. Bieniewska, B. E. Sauer, M. R. Tarbutt, A. Amy Klein, S. K. Tokunaga and B. Darquié, *Quantum Electron.*, 2019, **49**, 288–292.